

Dynamics of peptide capsules in saline solutions

by

Susan Katherine Whitaker

B.S., Kansas State University, 2014

A THESIS

submitted in partial fulfillment of the requirements for the degree

MASTER OF SCIENCE

Department of Biochemistry and Molecular Biophysics
College of Arts and Sciences

KANSAS STATE UNIVERSITY
Manhattan, Kansas

2018

Approved by:

Major Professor
John M. Tomich

Copyright

SUSAN K. WHITAKER

© 2018

Abstract

Nanocapsules have become more popular as potential therapeutic agents in recent years. Though liposomes are the most popular and well-studied, nanocapsules made of peptides have their distinct advantages as the research behind them intensifies. Branched Amphiphilic Peptide Capsules (BAPCs) are a type of self-assembling nanocapsules that are made up of two similar branched, amphiphilic, chemically synthesized peptides. These peptides self-assemble into bilayer delimited capsules capable of encapsulating solutes and even small proteins in aqueous solution. Previous studies have shown that these nanocapsules are taken up by cells in culture without negative effects and can be given to an organism, distributed throughout the organism without cytotoxic effects, suggesting a possible future as a therapeutic nanoparticle.

For use as a therapeutic system, the understanding of how these BAPCs behave in the presence of sodium and chloride, two very common biological ions, must be understood and characterized. Previously published work showed that the BAPC bilayer is semipermeable and excludes sodium and chloride ions. Current research has expanded on this. Besides being semipermeable, this bilayer is also a dynamic membrane that has the ability to expand and contract due to osmotic pressure from ions in solution. Eosin Y, an autoquenching dye, has been used for many of the studies to monitor the behavior and the amount of water within the BAPCs. Having insight into how the BAPCs change under physiological conditions is necessary if these nanoparticles are to be used in a clinical setting and may open doors to new uses.

Table of Contents

Abbreviations	vi
List of Figures	vii
Acknowledgements	viii
Dedication	ix
Preface	x
Chapter 1 – Introduction and Background	1
Self-Assembling Nanotechnology	1
Liposomes	2
Solid Lipid Nanoparticles	4
Polymersomes	5
Peptide-Based Nanoparticles	5
Branched Amphiphilic Peptide Capsules	8
Chapter 2 – Water-filled BAPCs in Varying External Solutions	17
Materials and Methods	17
Peptide synthesis	17
Peptide Cleavage and Deprotection	18
Preparation of Peptide Solutions	18
Fluorescence Assay of 5(6) Carboxyfluorecein in Variable pH	19
BAPC Formation with Eosin Y	20

Fluorescence Assays of Eosin Y BAPCs in NaCl	21
Circular Dichroism.....	22
Permeability of pH Variations in 5(6)Carboxyfluorescein-containing BAPCs	25
Results of Room Temperature BAPCs in NaCl	26
Eosin Y Room Temperature BAPC Fluorescence Studies	26
Room Temperature BAPC Circular Dichroism Studies	31
Results of Locked BAPCs in NaCl.....	34
Eosin Y Locked BAPC Fluorescence Studies	34
Locked BAPC Circular Dichroism Studies	39
Chapter 3 – Discussion and Future Work	42
Discussion.....	42
Future Work.....	47
References.....	50
Appendix A – Copyright Permissions	57

Abbreviations

BAPC	Branched Amphiphilic Peptide Capsule
Boc	tert-butyloxycarbonyl
CD	Circular Dichroism
CT	Computed Tomography
DHB	2,5-dihydroxybenzoic acid
DIEA	Diisopropylethylamine
DLS	Dynamic Light Scattering
DMF	Dimethylformamide
Fmoc	9-Fluorenylmethoxycarbonyl
FO	Forward osmosis
HATU	1-[Bis(dimethylamino)methylene]-1H-1,2,3-triazolo[4,5-b]pyridinium 3-oxid hexafluorophosphate
HOAt	1-Hydroxy-7-azabenzotriazole
HPLC	High Performance Liquid Chromatography
HPV	Human Papillomavirus
MALDI-TOF	Matrix-Assisted Laser Desorption Ionization – Time of Flight
MRI	Magnetic Resonance Imaging
MS	Mass Spectrometer
NMP	N-Methyl-2-pyrrolidone
PEG	Polyethylene Glycol
PET	Positron Emission Tomography
RES	Reticuloendothelial system
RO	Reverse osmosis
SEM	Standard Error of the Mean
SLN	Solid Lipid Nanoparticle
TFA	Trifluoroacetic Acid
TFE	Trifluoroethanol

List of Figures

Figure 1.1 – Sequences of h ₉ and h ₅ peptides	8
Figure 1.2 – Eosin Y fluorescence concentration curve	9
Figure 1.3 – CD spectra of BAPCs at 4°C, 25°C, and 37°C	10
Figure 1.4 – The fates of 25°C BAPCs.....	11
Figure 1.5 – Fluorescence intensity differences of DW- and NaCl-filled BAPCs	14
Figure 1.6 – Approximate normalized internal dye concentration	15
Figure 2.1 – Effects of pH on 5(6)Carboxyfluorescein in Solution and BAPCs.....	25
Figure 2.2 – Room temperature BAPCs in NaCl solutions	27
Figure 2.3 – Room temperature BAPC fluorescence values at 90 minutes.....	28
Figure 2.4 – Room temperature BAPCs back to water after NaCl.....	29
Figure 2.5 – Room temperature BAPCs initial versus final fluorescence	30
Figure 2.6 – Room temperature BAPC CD spectra.....	32
Figure 2.7 - Locked BAPCs in NaCl Solutions	34
Figure 2.8 – Locked BAPC fluorescence values at 90 minutes.....	35
Figure 2.9 – Locked BAPCs back to water after NaCl.....	36
Figure 2.10 – Locked BAPCs initial versus final fluorescence	37
Figure 2.11 – Locked BAPC CD spectra.....	41
Figure 3.1 - Room Temperature and Locked BAPCs Final Fluorescence	42

Acknowledgements

First and foremost, I would like to thank my major professor, Dr. John Tomich. He often had more faith in my ability than I did. I also send a thanks to my committee members, Dr. Michal Zolkiewski and Dr. Lawrence Davis. Throughout my undergraduate and graduate career at Kansas State University, I have learned a lot from them in many aspects.

I am also grateful to those current and past lab members who have been driving forces in my scientific development and success. I would especially like to thank Dr. Pinakin Sukthakar who did early work with the peptide capsules and has helped guide me through my research career. He instilled into me a love of laboratory work, a knowledge of peptide chemistry, and an experience that helped shape me into the researcher I am today. Other former lab members include Drs. Adriana Avila and Sheila Barros, and Jammie Layman. Also, I would like to thank Pavithra Natarajan, Ben Katz, and Kayla Wilkinson for their support and the current and former undergraduates who have directly contributed to my work: Mariah Brown, John Nail, Emily Wedeman, Macy Garcia, Jennifer Coats and Mark Brown.

Finally, I would like to thank my family, especially my husband, Michael, and my children, for their support, patience, and encouragement throughout these busy days and nights.

Dedication

I would like to dedicate this work to my family who have given me the support and the drive to continue in school and succeed.

Preface

When I started with the preliminary work BAPCs five years ago, I couldn't have imagined I would have come to where I currently am. I have gained a great appreciation and respect for the nano-scale world around me and what it can mean for the future of research, technology, and so many other fields.

I could not have made it as far as I have without an amazing support of fellow lab members, peers, and family. I appreciate the hard work and sacrifices that everyone has made to help me get to where I am now.

Chapter 1 – Introduction and Background

Self-Assembling Nanotechnology

Nanotechnology and nanocapsules are those molecules or assembled particles that are less than 100 nm in diameter.^{1,2} Cells, being micrometers in diameter dwarf these nanoparticles. This small size allows them to be taken up by cells, but large enough to act as a drug delivery vehicle for therapeutic agents, suggesting future applications in basic research and clinical applications. Over the past 10 years, the field of nanotechnology and the use of nanoparticles and nanocapsules have become much more popular and a more attractive option for many applications. This can be seen by the increase in number of patents that have been issued for nanoparticles and nanocapsules, and the NIH has been increasing the funding for research being done with nanotechnology in the past 10 years.^{3,4}

Nanocapsules and nanoparticles come together via self-assembly, typically in aqueous solvents, and are held together non-covalently. Since their discovery, they have seen potential applications in material science, electronic devices, and chemical science with many of these nanoparticles designed with various clinical applications in mind.⁵ These could be used as a drug delivery system-especially for drugs that are hydrophobic or highly toxic, tissues or organ repair, cancers or other disease diagnostics, or vaccine delivery.^{6,7,8,9} With a maximum size of 6 nm for solutes that can pass through kidneys, nanocapsules can also be used to protect proteins, peptides, or other therapeutics from degradation or elimination from the body. This allows for increased circulation times thus giving the nanoparticles more time to reach the target cells and could even increase patient compliance. By increasing the stability and availability and decreasing degradation, the door could be opened to possible delivery mechanisms that were

previously not able to be accomplished, such as the effective oral delivery of protein and peptide drugs.^{10,11,12,13}

One of the most hopeful areas of nanotechnology is in the area of specialized cancer treatment and detection.^{6,7,14,15} Cancer is a leading cause of death, and the number of new cases is only expected to rise.^{16,17} Many of these nanocapsules can encapsulate poorly soluble or highly toxic drugs and deliver them to the desired cell for maximum therapeutic efficacy and decrease off-target side effects. Most currently approved nanocapsules and nanotechnologies used in therapeutics do not target specific cells, but they accumulate in tumor tissues due to the physiology of the tumors. The nanocapsules with a diameter as large as 200 nm can easily go through the leaky vessels around tumors, thereby passively targeting the malignant tissues.¹⁸ The hope and direction of development for these nanocapsules is for coating them with specific targeting molecules. By putting these specific epitopes, peptides, or small molecules on the surface of them either covalently-via disulfide bonds or NHS-linkage-or non-covalently-via electrostatic interactions or streptavidin-biotin conjugation-they can directly target the tumor cells for imaging or destruction.^{19,20} The future of nanotechnology is quite bright, and nanotechnology lends itself perfectly to be used in early and more accurate cancer detection-like use as adjuncts to CTs or X-rays, MRIs, PET scans, and ultrasound, better cancer treatment options, and cancer research along with use in many other areas of research, delivery, and therapeutics.^{1,4,12,21,22}

Liposomes

Liposomes are the most commonly seen nanoparticle, and these were one of the first nanocarriers approved for medicinal use by the FDA in 1995.^{1,23,24} In the last thirty years, the

development and use of liposomes has sharply increased, especially in the field of pharmacology, and the use of liposomes approved for use in medicine has shown that they are effective.²⁵ Composed of a lipid bilayer, liposomes can self-assemble within aqueous solvents, encapsulating various solvents and solutes within them or even within the bilayer.^{23,25} Using a liposome as a delivery vehicle for pharmacological agents has a number of advantages. First, liposomes are biodegradable and compatible with biological systems. Because of their compatibility with these systems, they can be predictably modified to retain or release cargo at certain conditions.²⁶ Next, depending on how they are made, the sizes of the nanoparticles can also be tuned to a specific size and release the drug within it at certain conditions (e.g. temperature or pH).²⁴ Moreover, when liposomes are used as part of a therapeutic drug, they can lengthen the time of circulation of the drug, aid in drug delivery to the inside of the cell, increase the efficacy of the drug, and have decreased side effects from the drug.^{23,27,28} Many of the drugs used are not readily soluble in solvents used for delivery of medications, so liposomes also solubilize these hard to dissolve molecules.^{27,29}

As mentioned previously, liposomes, like other nanoparticles, are being modified to contain specific molecules on the external surface of the capsule. Liposomes have been coated with polyethylene glycol (PEG). This coating of PEG prevents premature destruction by the organism's immune system through the reticuloendothelial system (RES). Liposomes can be easily modified in other ways to have ligands or other targeting molecules or peptides on the outside of them to aid in correct delivery of their cargo to the desired cells.^{23,26}

Liposomes as delivery vehicles are not without drawbacks. First, the use of liposomes is limited in therapeutics due to their short shelf life once they are prepared.^{24,28} If they are recognized by the immune cells, they can be taken up and inactivated by the RES. This

drastically cuts the circulating time of the liposomes and the efficacy of the therapeutic they are attempting to deliver. Liposomes have even been shown to induce a complement activation of the immune system in rats and pigs.^{1,23} Besides these specific immune responses, liposomes, especially the cationic liposomes, can cause blood clots. Structurally, permeability and integrity of the liposome bilayer can change based on the external conditions. Under conditions such as high pressure or temperature, liposomes can leak their internal solutes through the bilayer or fenestrations can develop within the bilayer, making the bilayer permeable to external solutes and solvents.²⁶

Solid Lipid Nanoparticles

Other nanoparticles, nanocapsules, and nanocarriers have been developed, some of which are structurally similar to liposomes. Solid lipid nanoparticles (SLN) are composed of lipids and can contain the molecule or therapeutic drug within the small pores inside of them. An advantage these have over liposomes is their longer shelf life.²⁴ The sizes of these can also vary, depending on how they are made, meaning they can also have a wide range of uses therapeutically. Much like liposomes, SLNs can be tuned to release their cargo at defined pH or temperature values.²⁴ Though the hydrophobicity of them can vary somewhat, SLNs are typically hydrophobic in the core as compared to the aqueous-filled core of the liposome. This may mean that many aqueous solvents and hydrophilic solutes used therapeutically do not mix well with them, thereby limiting their usefulness.²⁴

Polymersomes

Another nanocarrier that has been developed is the polymersome. These have different polymers, often times with blocks of repeating subunits within them, as their base units, and have been called block copolymers.³⁰ These block copolymers have increased in use and development significantly over the past 10 years. Despite being different with respect to the base units as compared to liposomes, these show some structural similarities to liposomes. Encapsulation of the solutes and solvents within a hydrophilic core is similar to the structure of liposomes. These block copolymers have been shown to be much more stable than liposomes, especially in high concentrations above the critical micelle concentration (CMC) and when cross-linkers are used to stabilize the structure.³² The content within them can also be released more specifically than is seen with liposomes and their size and thickness can be easily modified depending on the composition of the polymer.^{30,31}

These block copolymers are also not without their disadvantages. Though the polymers within them are typically non-toxic, they can contain other compounds or components within them which can be toxic when delivered in vivo.³¹ These toxic compounds are typically the molecules that are used to increase stability and cross-link the copolymers together. Constructing these block copolymers into the functional nanoparticles can also take more time and energy with than other nanoparticles and nanocarriers, making them not very cost-effective to use in large quantities.^{25,30,32}

Peptide-Based Nanoparticles

Another type of nanoparticle is that made from organic molecules, such as a peptides or proteins that can self-assemble into nanocapsules.³³ These nanocapsules are made from mainly

the natural amino acids and have many advantages over the traditional liposome delivery system.^{18,21} These peptide nanoparticles have a sequence that has been derived from a peptide or protein sequence or developed from de novo design.³³ By making these therapeutics out of peptides that form nanocapsules, the problematic limited bioavailability, poor biodistribution, instability, and short half-lives that are seen with free peptides, especially in the more harsh conditions in the body, can be greatly decreased.^{18,21,34} Also, because they are made from natural amino acids, they are non-toxic to the organism upon breakdown.¹⁸ Typically, these peptide-based nanocapsules are assembled non-covalently. This means that they are self-assembled using hydrophobic interactions, van der Waals interactions, hydrogen bonding, π - π stacking, and electrostatic interactions to make these nanoparticles more tunable to rupture at certain conditions.^{18,35}

Like other nanoparticles, peptide-based nanoparticles also have distinct advantages. Many of these peptide-based molecules are typically easy to modify based on the well-known chemistry of many of the reactions. For example, these peptide-based systems can be easily modified or “tuned” by changing the sequences, by changing the amino acids from L to D conformations, or by the addition of carbohydrates, fatty acids, or other molecules onto the peptides.^{17,21,36,37} These modifications can also be made to either intentionally elicit or avoid an immune response within the organism, much like was discussed with PEG on liposomes. The molecule used would depend on the desired effect-whether it is to deliver a therapeutic where minimal immune response is desired or to make a vaccine where more of an immune response is required.^{17,21}

Other molecules can be easily added to decorate the outside of the nanocapsules to direct the capsule where to go in vivo. These areas that can be targeted with peptide-based drugs

include the central nervous system, cardiovascular tissue, bones, and tumors, all of which are locations that are often difficult to target with other therapeutic systems.^{17,21,38} This specific targeting has been an area of research and therapeutics that has increased sharply over the past few years.¹⁸ Peptide-based nanoparticles are also very stable, easy to make in large quantities, have less extensive assembly preparation, are biodegradable, and are compatible with many organisms.

Peptide nanoparticles can also be used as vectors for gene delivery. Because the DNA or RNA is not able to cross the cell membrane on its own, a vector is needed. These delivery vehicles may be viral or non-viral, and the peptide carriers fall under the latter.^{36,39} The viral vectors, no matter how modified they have been, still have downfalls such as limited carrying capacity, limitations of the types of oligonucleotides they can deliver, incompatibility with human genetics, and potentially causing an unintentional immune response.^{2,36} These limitations can be avoided by using peptide delivery vehicles, including peptide nanocapsules. The nanocapsules, unlike viral delivery vectors, can easily be prepared in large quantities and have the potential for lower toxicity and fewer side effects.² These peptide delivery systems require that the negative charges on the different kinds of DNA or RNA are neutralized or masked, which many peptides, especially cationic peptides with lysine and arginine, can do.^{20,36,40} The degradation of the oligonucleotide must also be prevented, and by either covalently attaching them to peptides, encapsulating them within peptide nanocapsules, or otherwise affixing them to peptide nanocapsules, the oligonucleotides can be transported intact to and into the desired cells often using endocytosis.^{2,36,40} Though there are no nanoparticle gene delivery systems approved by the FDA yet, many are working on developing, testing, and advancing these peptide-based nanoparticles for use for gene delivery.²

Branched Amphiphilic Peptide Capsules

An example of a peptide-based nanocapsule is Branched Amphiphilic Peptide Capsules (BAPCs). These branched peptides were first described in Gudlur et al.⁴¹ These self-assembling nanocapsules are formed from a pair of branched, chemically synthesized peptides which were modified from a known calcium channel peptide sequence. These peptides have a similar structure to diacyl glycerol molecules; they have amphiphilic character with a polar end composed of positively charged lysine residues and a hydrophobic end composed of two tails (Figure 1.1). Because of the high percentage of hydrophobic amino acids in each tail, for either

the 9 or the 5 amino acid residue tails (Figure

1.1) these peptides were termed h₉ and h₅

respectively. Early work done by Gudlur et

al⁴¹ showed that these nanocapsules could

encapsulate fluorescent dyes and other solutes

in aqueous solutions but were unstable in

organic solvents such as trifluoroethanol.

Coarse-grained modeling supported the idea that they formed nanocapsules.

Once documented that this peptide pair self-assembled to form peptide-based nanocapsules, further biophysical and structural characterization was done to explore how the BAPCs behaved under different conditions. Using electron microscopy, the sizes of the nascent and mature BAPCs were determined. Once the branched peptides h₅ and h₉ are combined in equimolar amounts and hydrated with water, they immediately begin to form what appears to be nano-fibrils. However, by 30 minutes, capsules with a diameter of about 20-30 nm formed. By 2

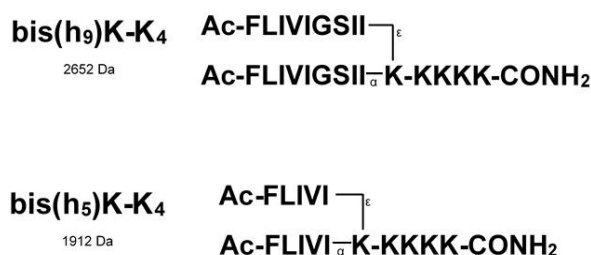


Figure 1.1 – Sequences of h₉ and h₅ peptides

Shown are the sequences of the self-assembling branched peptides h₉ and h₅. The branch point occurs on the fifth lysine residue with branches coming off at amine groups on the N terminus and the ϵ amine of the side chain.

hours at room temperature, the sizes of the BAPCs have increased up to 500 nm, suggesting the individual BAPCs underwent fusion thereby significantly increasing their size.⁴²

In order to understand how these BAPCs behaved, fluorescent dyes were used, and one dye was found to be paramount in the characterization of the BAPCs: Eosin Y. First described in Sukthankar et al⁴², Eosin Y shows a predictable change in fluorescence based on the concentration of the Eosin Y in solution (**Figure 1.2**). The fluorescence increases with the concentration of Eosin Y until the concentration reaches about 150 μM . As the concentration of the dye increases further, the fluorescence decreases suggesting that the other molecules of Eosin Y begin to self-quench the fluorescence intensity.³⁶ Because of the predictable fluorescence changes seen with small concentration changes of Eosin Y, this became an ideal dye for use within the BAPCs.

In Sukthankar et al⁴², Eosin Y at a concentration of 2.126 mM in water was encapsulated

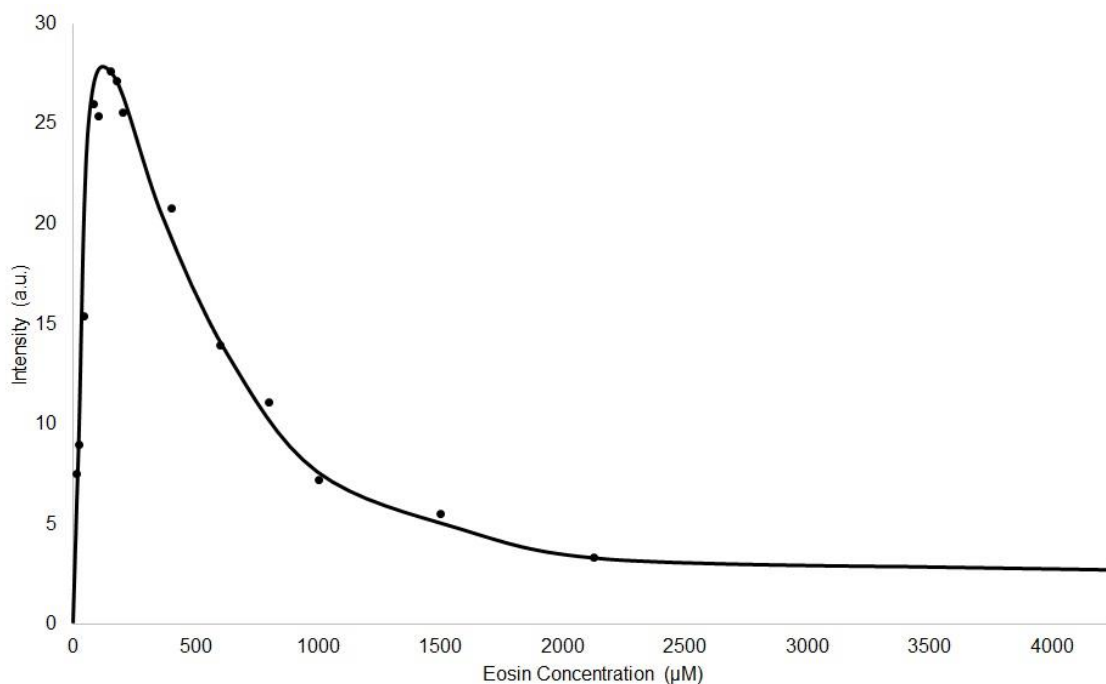


Figure 1.2 – Eosin Y fluorescence concentration curve

The points show the maximum Eosin Y fluorescence intensity at increasing concentrations of Eosin Y in distilled, deionized water. (Excitation wavelength: 490 nm; emission range scanned: 495 to 800 nm; quartz cuvette with 0.3 cm path length; scan rate: 600 nm/min; PMT detector voltage: 600 V; excitation slit: 2.5 nm; emission slit: 2.5 nm)

within BAPCs. These Eosin Y filled BAPCs were mixed with a 20X population of water-filled BAPCs, and the fluorescence was monitored. Over time, the fluorescence increased steadily

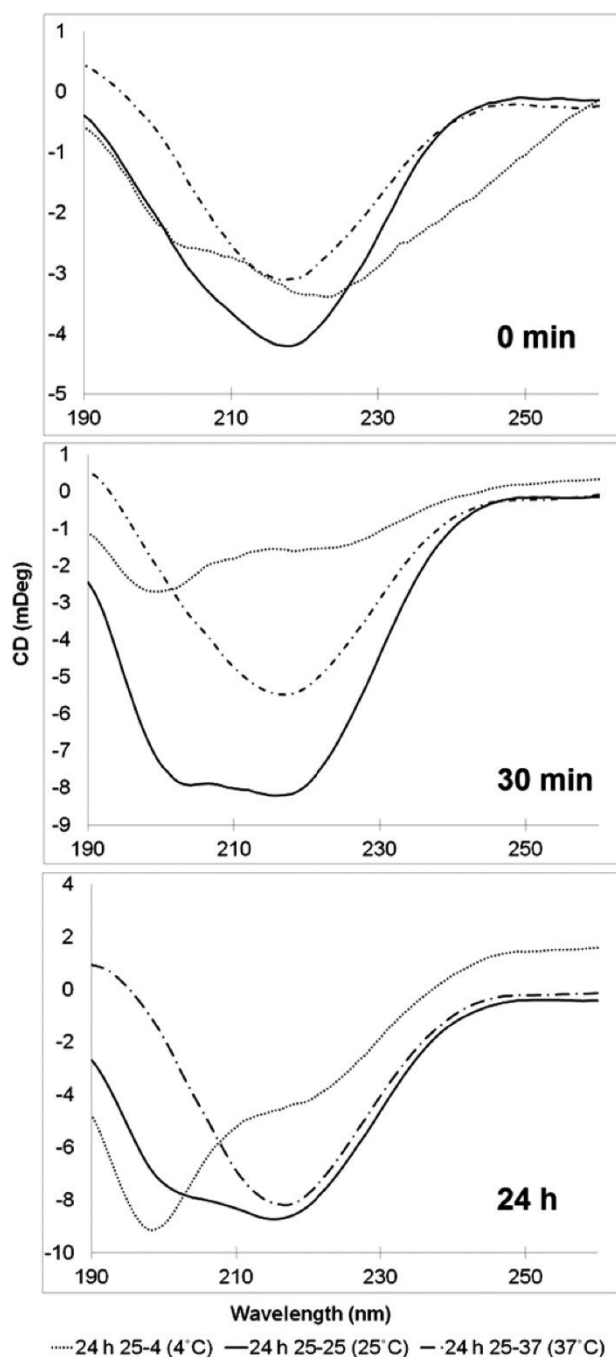


Figure 1.3 – CD spectra of BAPCs at 4°C, 25°C, and 37°C
The CD spectra of the BAPCs with equal molar concentrations of h₅ and h₉ peptides. All were made at 25°C and moved to either 4°C or 37°C after 30 minutes or kept at 25°C. Reprinted with permission from reference 43. Copyright 2015 American Chemical Society.

indicating that the Eosin Y dye within the BAPCs was becoming more diluted over time. In order for this to happen, the BAPCs had to be fusing thereby mixing the contents of the water-filled and Eosin Y-filled BAPCs. This data correlates with the earlier electron microscopy data that showed that BAPCs increased in size due to fusion. This work with the BAPCs and Eosin Y illustrated the usefulness of Eosin Y in the studies of BAPC characterization.⁴²

Further characterization studies were published in Sukthankar et al.⁴³ These studies looked at the circular dichroism (CD) spectra to determine the secondary structural characteristics of the peptides as they move through different temperatures (**Figure 1.3**). It was seen that BAPCs composed of h₅ and h₉ together and brought to 4°C almost

immediately adopt a more random coil composition. As the BAPC solutions were warmed to 37°C, the peptides develop more β -sheet composition. The peptides at room temperature show a mix between β -sheet and random coil characteristics in the CD.⁴³

In Sukthankar et al,⁴³ there was a conformation of BAPCs also identified and characterized. These BAPCs are made at room temperature and taken to 4°C before being brought back to room temperature. These BAPCs have been shown to resist the TFE-induced rupturing that is seen with BAPCs made at the other temperatures, and because of this, these BAPCs were named “locked BAPCs”. Using Eosin Y and water BAPCs as previously done, it was seen that these locked BAPCs did not fuse as the BAPCs made at room temperature do, even when brought to 80°C. This also showed that small temperature changes can change the BAPCs’ characteristics and behavior (**Figure 1.4**).⁴⁴

Like many other peptides and nanocapsules previously discussed, BAPCs are also able to penetrate the cell membrane. Upon being taken up by HeLa cells in cell culture, they remained in HeLa cells for at least two weeks without rupturing. Distinct fluorescent dye-filled capsules can be seen in both the parent cells

and the daughter cells. Experiments using temperature changes and BAPC uptake showed that the entry into the cells occurs via the endosomal pathway. These BAPCs then escape the late endosome, most likely due to their positive

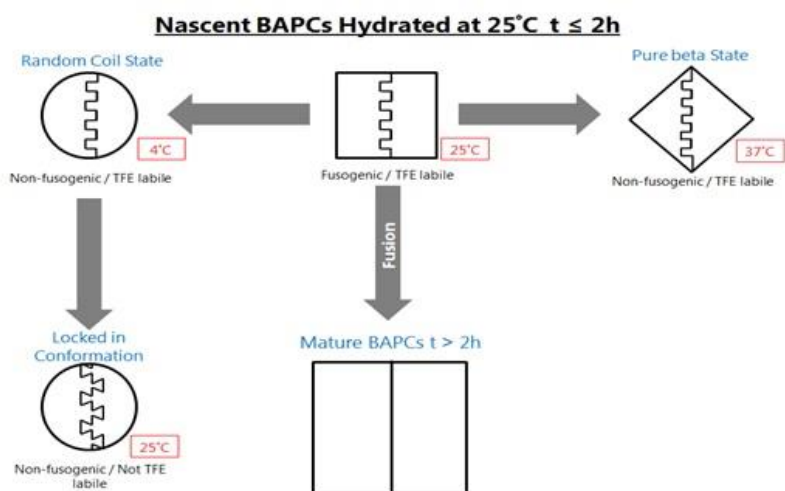


Figure 1.4 – The fates of 25°C BAPCs

All temperature-induced states are irreversible. It was found that the BAPCs hydrated with 4°C or 37°C water form uniform 20-30 nm non-fusogenic capsules that rupture in the presence of TFE. Reprinted with permission from reference 43. Copyright 2015 American Chemical Society.

charges of the many lysine residues and the proton-sponge effect.^{44,45,46}

BAPCs have also shown biocompatibility, which is a benefit of peptide capsules, and preliminary studies have shown a potential use for therapeutics. The first study that showed their potential use in therapeutics was seen when ^{225}Ac -loaded BAPCs were injected into mice. As the ^{225}Ac degrades to ^{213}Bi , daughter alpha particles are released with retention of the daughter radionuclides. Alpha-emitting isotopes can cause damage to chromosomes. Liposomes must be much larger (too large to be useful) than the BAPCs to overcome the powerful recoil of the daughter radionuclides. This rupture does not occur with the BAPCs, though. This shows that they are taken up by many different cells within different tissues and can withstand a great deal of force and still remain intact. This also shows benefits to these capsules as a delivery vehicle and therapeutic aide as compared to the more traditional liposome.⁴⁴

Another in vivo study was done in Avila et al⁴⁷ using the BAPCs as a delivery vehicle for DNA vaccines into mice. From previous work, it was known that when locked BAPCs and DNA were combined in the appropriate N:P ratios (N being the NH_3^+ on the lysine residues and P being the PO_4^- on the DNA), the DNA and BAPCs would form a complex. These BAPCs associated with the DNA would then help the DNA become internalized within the cell and transfect the cells with the new genetic material.⁴⁸ After the mice were injected with these BAPCs to deliver the viral DNA from a North American type I porcine and reproductive syndrome virus, competent RNA viruses were actually shed. This shows that the genetic material can effectively be delivered to an organism without damaging the DNA. Also in this paper, mice had DNA:BAPC complexes composed of an HPV E7 containing DNA plasmid. Those mice that received the DNA with the BAPCs lived longer and had smaller tumors than those who did not have the BAPCs used.⁴⁷ These recent studies in mice suggest that there is a potential for future in

vivo use of these BAPCs, but there had not been much work on how these BAPCs behaved in the presence of physiologically pertinent ions like sodium and chloride.

The interaction with water and ions was first discussed in Jia et al.⁴⁹ Using molecular dynamics simulations, water was shown to flow freely and spontaneously through the bilayer without lingering between the peptide leaflets. It can be suggested that the water molecules form hydrogen bonds with the peptide backbones of the hydrophobic regions of the peptide. This allows the water molecules to move readily and rapidly, even throughout the hydrophobic tail regions. When these simulations were done with the presence of sodium or chloride ions, it showed that they did not readily cross the bilayer as the water did during the simulation time.

The selective movement of water but not ions that was seen in the molecular dynamics simulations was also seen in experiments with BAPCs with either Eosin Y or Rhodamine 6G dyes. These dyes are negatively or positively charged, respectively, and Rhodamine 6G has a fluorescence concentration curve nearly identical to the autoquenching curve of Eosin Y shown in **Figure 1.2**. BAPCs were formed with 2.216 mM Eosin Y or Rhodamine 6G dye within them. This dye was in a solution of distilled, deionized water or NaCl (concentrations of 20, 50, 100 or 300 mM). The BAPCs containing dye and distilled, deionized water were divided in half. One half was suspended in water and the other half was suspended in 1 M NaCl. The fluorescence of these solutions were taken immediately after suspension in the water or NaCl. The BAPCs containing dye and NaCl were treated similarly. They were suspended in the isotonic solution of NaCl in which they were made and also suspended in distilled, deionized water. Fluorescence readings were taken immediately after suspension of these BAPCs as well. The fluorescence values of the BAPCs in the isotonic solutions were subtracted from the fluorescence values of the BAPCs in the hyper- or hypotonic solutions. The resulting values can be seen in **Figure 1.5**.

The bars that extend below the zero point in the graph show fluorescence values that are smaller after they are moved to the NaCl solution. This decrease in fluorescence suggests that the Eosin Y and Rhodamine 6G dyes within

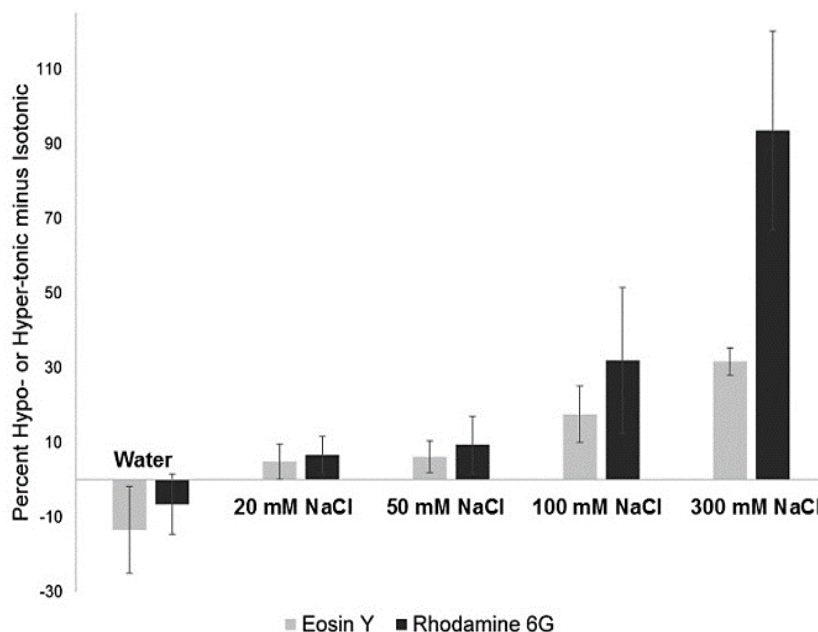


Figure 1.5 – Fluorescence intensity differences of DW- and NaCl-filled BAPCs

Shown are the fluorescence values of the BAPCs in hypo- or hypertonic solutions minus the fluorescence of the same BAPCs in the isotonic solutions. Shown are Eosin Y and Rhodamine 6G-containing BAPCs made to encapsulate increasing concentrations of NaCl along with the dye. The NaCl concentrations are shown on the horizontal axis and the difference in percent is shown on the vertical axis. It is suggested that the change seen between Rhodamine 6G and Eosin at high salt concentrations may be due to the large fluorescence changes seen with Rhodamine 6G in NaCl. Error bars represent standard error of the mean with $n \geq 3$. Reprinted with permission from reference 49. Copyright 2016 American Chemical Society.

due to osmotic changes in the solution surrounding them. The bars that extend above the zero line in the graph show fluorescence values that are greater once the BAPCs containing NaCl-dye solution are moved into water. This data seems to show that water is also moving into the BAPCs in a NaCl concentration dependent manner. After the external solutions were changed, the BAPCs were then filtered again and the flow-through was checked for fluorescence. This flow-through did not have any detectible fluorescence, suggesting that all of the fluorescence changes were from inside of the BAPC, not from dye released into the solution outside of the BAPC, and the BAPCs remained intact and stable through the changes of saline concentration.⁴⁹

When these relative changes in Eosin Y fluorescence are plotted on a fluorescence curve of Eosin Y, the approximate final concentrations, and therefore the approximate sizes, can also be estimated (**Figure 1.6**). By assuming that the beginning BAPC that contains 2126 μM Eosin Y is 20 nm in diameter, the following could be calculated: 5000 μM Eosin Y is 15 nm diameter, 1375 μM Eosin Y is 23 nm in diameter, 1250 μM Eosin Y is 23.9 nm in diameter, 800 μM Eosin Y is 27.7 nm in diameter, and 500 μM Eosin Y is 32.4 nm in diameter. All of these numbers are within the known limits of the sizes of these capsules, which shows that it these numbers are not

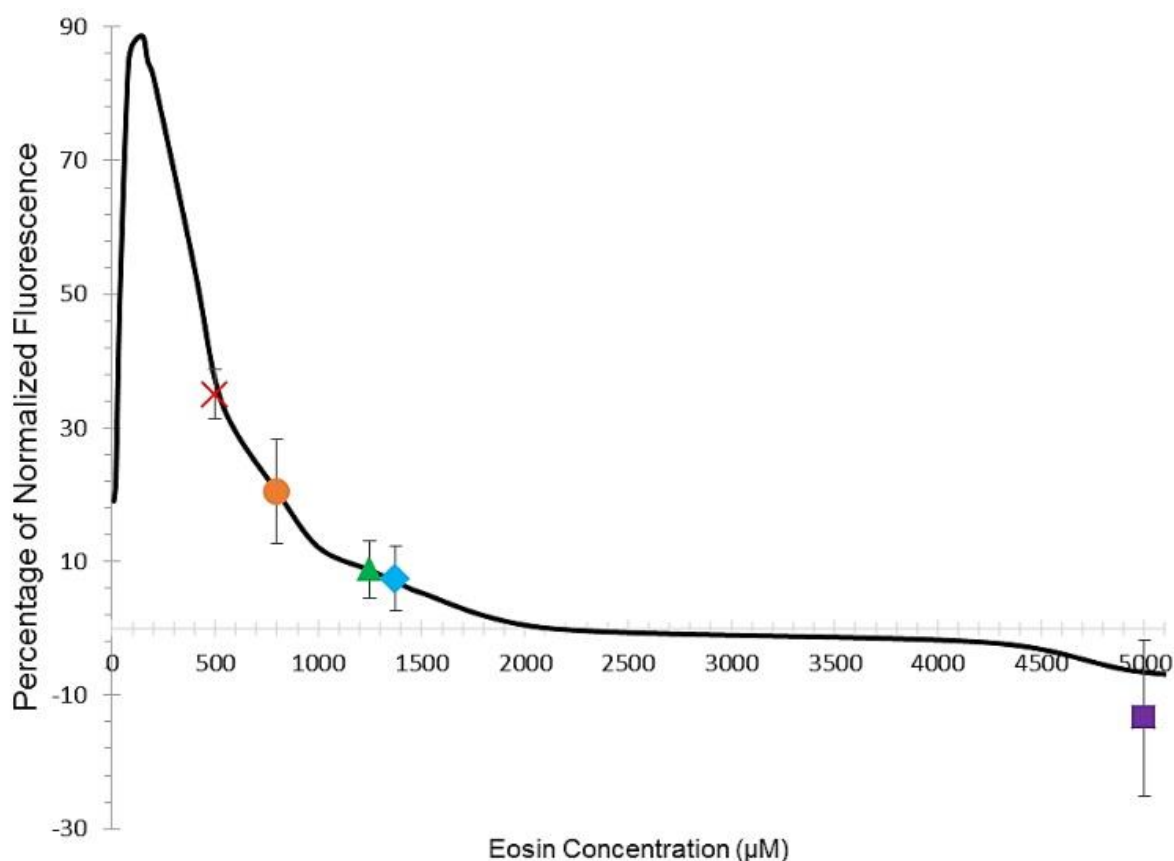


Figure 1.6 – Approximate normalized internal dye concentration

The line shows the average Eosin Y fluorescence at increasing concentrations. The scanning parameters were the same as used in **Figure 1.2**. To find the normalized fluorescence, each fluorescence intensity was calculated as a percent of the maximum. The value at 2126 μM was subtracted from each. The marked points on the graph show approximate locations where percent fluorescence values from the NaCl or water BAPCs seen in **Figure 1.5** fall on this line. (Red X = 300 mM NaCl BAPCs; Orange Circle = 100 mM NaCl BAPCs; Green Triangle = 50 mM NaCl BAPCs; Blue Diamond = 20 mM NaCl BAPCs; Purple Square = Water BAPCs). Error bars represent SEM and $n \geq 3$. Reprinted with permission from reference 49. Copyright 2016 American Chemical Society.

outside of the realm of possibility. This data suggests that the BAPC bilayer can act as a semi-permeable membrane allowing ions and solvents to remain on one side while water passes freely through instantaneously.⁴⁹

Chapter 2 – Water-filled BAPCs in Varying External Solutions

Materials and Methods

Peptide synthesis

The h₅ and h₉ peptides were synthesized on an ABI 431 automated peptide synthesizer using Fmoc chemistry on 0.1 mmol scale using CLEAR amide resin (Peptides International, Louisville, KY). All amino acids were N-Fmoc protected amino acids (P3 Biosystems, Louisville, KY and AnaSpec, Fremont, CA) and used at 0.5 mmol per synthesis. The N-terminal lysines were double coupled, and the branch point was introduced into the sequence by using a lysine with an Fmoc protecting group on both the α - and the ϵ -amino groups as compared to the Boc protecting groups on the ϵ -amino groups on the other lysines. The amino acids of the hydrophobic tails were all triple coupled. Piperidine (99% Purity, Sigma-Aldrich, St. Louis, MO) was used in NMP to remove the Fmoc and deprotect the amino-terminal groups. Activation of each amino acid was done using a solution of 0.225 M HOAt/HATU in DMF. After the final amino acid was added and the Fmoc removed, the amino terminus was protected using acetyl anhydride. For h₉ only, the initial lysine was added off of the peptide synthesizer, activated, and only allowed to react for five minutes. Once the five minute was completed, the resin was rinsed with NMP and capped with the acetyl capping cocktail to block any other unoccupied active sites on the resin. The remainder of the synthesis was completed as described above on the automated peptide synthesizer. This method is used to eliminate sterically inaccessible sites on the resin that could eventually result in numerous failed sequences by the time the last amino acid was added.

Peptide Cleavage and Deprotection

The peptides were cleaved from the resin using a solution of 98% TFA and 2% distilled, deionized water. This was mixed at room temperature for 90 minutes in order to cleave peptide from resin and remove protecting groups from amino acid side chains. The slurry was put through a filter and the liquid poured into ice cold diethyl ether to precipitate peptide. The peptide was then washed with diethyl ether three times. The h₅ peptide was then suspended in distilled deionized water and lyophilized. The h₉ peptide was dried directly from the diethyl ether without suspending in water. Adding h₉ to water results in its adopting β -structure leading to the formation of insoluble aggregates. Once dried, the peptide was analyzed using reverse phase HPLC on a Beckman machine running 32 Karat (version 8.0) software with a C18 column (Buffer A: 99.9% water and 0.1% TFA; Solvent B: 90% Acetonitrile, 9.9% water, and 0.1% TFA) with a 10% to 90% Buffer B gradient over 30 minutes. MALDI-TOF MS was also used for analysis with the peptide spotted in a DHB matrix (Sigma-Aldrich, St. Louis, MO) on a Bruker Ultraflex II machine.

Preparation of Peptide Solutions

Once peptides were dried, a small amount of each was dissolved in 100% TFE and absorbances were taken at 257.5 nm in a 0.3 cm path length quartz cuvette (Cary UV/Vis Spectrometer, Varian Inc., Palo Alto, CA). Using Beer's Law where $A = \epsilon cl$ (A =absorbance, ϵ =molar extinction coefficient (195 M⁻¹cm⁻¹ for Phe at 257.5 nm), c =concentration of the solution, l =pathlength of the cuvette), the precise concentration of the peptides the TFE solution could be determined from the absorbance values of the phenylalanine of the peptides in solution. From this, 300 μ L of 1 mM concentration of both h₅ and h₉ were combined and dried in a new

tube in the Speedvac, unless another concentration and volume were specified. These were made within one or two days of use as this showed the most consistent results.

Fluorescence Assay of 5(6) Carboxyfluorescein in Variable pH

The peptides were combined and prepared as described above but instead equimolar concentrations of 5 mM each peptide were used. Once dried, they were hydrated in a drop-wise fashion with 200 μ L of 4°C 1.5 mM 5(6)Carboxyfluorescein (Sigma-Aldrich, St. Louis, MO) dissolved in water. These were moved to 4°C for another 30-45 minutes. .

After this incubation time, the BAPC plus peptide solutions were transferred to an Amicon Ultra-0.5 mL centrifugal cellulose filter with 30 kDa molecular weight cut-off (EMD Millipore, Billerica, MA) and centrifuged at 14000 x g for 5 minutes in an Eppendorf 5415 D benchtop centrifuge. External dye passed through the filter while the 5(6)Carboxyfluorescein-containing BAPCs remained in the filter.

The BAPC solution retained in the filter was washed twice with a 300 mM solution of Na-TFA (Sigma-Aldrich, St Louis, MO) in distilled, deionized water solution to remove any externally-bound dye molecules. The BAPCs were then washed with water to remove any additional external dye from the solution around the BAPCs. The filters were then inverted into clean tubes and centrifuged at 2000 x g for 5 minutes to remove the BAPCs from the filters. The recovered retentate was then divided into two equal amounts into clean tubes for fluorescence analysis.

The two samples were then suspended in either pH 2 HCl and distilled, deionized water or 100 mM pH 9 Tris Buffer and distilled, deionized water. Fluorescence was obtained on a CARY Eclipse fluorescence spectrometer (Varian Inc., Palo Alto, CA, scan rate: 600 nm/min;

PMT detector voltage: 600 V; excitation slit: 5 nm; emission slit: 5 nm). An excitation wavelength of 492 nm was used and the fluorescence was obtained from 500 to 700 nm within a 0.3 cm path length quartz cuvette. Solutions of 37.5 μ M 5(6)Carboxyfluorescein were also made within the solutions of pH 2 HCl, distilled, deionized water, or 50 mM pH 9 Tris Buffer. These were scanned as above with the exception of the excitation and emission slits of the CARY Eclipse being 2.5 nm for the dye solutions.

BAPC Formation with Eosin Y

Once dried from TFE solution, the 1 mM/300 μ L h₅h₉ peptides were hydrated in a drop-wise fashion with 300 μ L of a room temperature solution of 2.126 mM Eosin Y (Sigma-Aldrich, St. Louis, MO) dissolved in water. To make room temperature BAPCs, the tubes were allowed to sit at room temperature for 30-45 minutes without mixing and filtered as described below.

To make locked BAPCs, the BAPCs were hydrated with 300 μ L of a room temperature solution of 2.126 mM Eosin Y solution. After 30-45 minutes, the tubes were moved to 4°C for at least 30-45 minutes. The BAPC solution was then removed from 4°C and brought back to room temperature by sitting on the benchtop for an additional 30-45 minutes.

Once the incubation time was completed, the dye plus peptide solutions were passed through a pre-wet 0.22 μ m PTFE syringe-driven filter (EMD Millipore, Billerica, MA) to remove the larger dye-peptide aggregates. This was put directly into an Amicon Ultra-0.5 mL centrifugal cellulose filter with 30 kDa molecular weight cut-off (EMD Millipore, Billerica, MA) and centrifuged at 14000 x g for 5 minutes in an Eppendorf 5415 D benchtop centrifuge. BAPCs in solution were retained in the filter while any external dye was passed through the filter.

The retained BAPC solution was washed twice with a 300 mM solution of Na-TFA (Sigma-Aldrich, St Louis, MO) in distilled, deionized water solution in order to remove any externally-bound dye molecules. The BAPCs were then washed with water at least four additional times to remove the salt solution and any additional dye molecules from the solution around the BAPCs. The filters were then inverted into clean tubes and centrifuged at 2000 x g for 5 minutes to remove the BAPCs from the filters. The recovered retentate was then divided into two equal amounts into clean tubes for fluorescence analysis.

Fluorescence Assays of Eosin Y BAPCs in NaCl

One half of the BAPC solution filtered through the Amicon Ultra-0.5 mL centrifugal cellulose filters with 30 kDa molecular weight cut-off filter was suspended in 300 μ L distilled, deionized water and the fluorescence was scanned on a CARY Eclipse fluorescence spectrometer (Varian Inc., Palo Alto, CA, scan rate: 600 nm/min; PMT detector voltage: 600 V; excitation slit: 10 nm; emission slit: 10 nm). An excitation wavelength of 500 nm was used and the fluorescence from 505 to 700 nm within a 0.3 cm path length quartz cuvette was obtained. The other half of the solutions were resuspended in NaCl solutions of either 10, 20, 50, 100, or 300 mM NaCl and fluorescence measurements taken as described above immediately after addition of NaCl solution and every 2 minutes over 90 minutes. Once these scans were completed, the BAPC solution from the cuvette was transferred back into an Amicon Ultra-0.5 mL centrifugal cellulose filter with 30 kDa molecular weight cut-off filter and centrifuged at 14000g for 5 minutes. The filter was then inverted into a clean tube and spun again at 2000g for an additional 5 minutes to remove the BAPC solution from the filter. This BAPC solution was then resuspended in 300 μ L

water and fluorescence measurements taken immediately after the addition of water and every 2 minutes over 30 minutes.

The values at 538 nm were taken from each run and the values were adjusted to account for the blank – the change in fluorescence of BAPCs suspended in pure water and treated in the same manner. Each NaCl concentration was repeated at least three times. Percent change from water was then calculated and the starting time zero value was normalized to 100% for the BAPCs in the salt solutions. For the BAPCs that were put back into water, the final scan was taken to equal 100% and the other values of the scans were taken as a percentage of that.

Circular Dichroism

For circular dichroism (CD) studies on the BAPCs, peptide concentrations were measured as previously discussed and 2 mM/150 μ L of both h₅ and h₉ were used for these studies. These peptide solutions were hydrated with 150 μ L distilled, deionized water at room temperature and allowed to sit for 30-45 minutes. For the locked BAPCs, the BAPCs were hydrated with the 150 μ L of room temperature distilled, deionized water and allowed to sit at room temperature for 30-45 minutes. Then, the tubes were moved to 4°C for at least 30-45 minutes. The BAPC solution was then brought back to room temperature by allowing the tubes to sit on the benchtop for an additional 30-45 minutes.

After the incubation time was completed, the solution was divided equally into two tubes. To one of the tubes was added 75 μ L distilled, deionized water, and the absorbance of this was taken at 257.5 nm as discussed in the section **Preparation of Peptide Solutions**. The CD spectra of the BAPC solution in water were obtained from 260-190 nm at 50 nm min⁻¹ with 1 nm step

intervals using a Jasco J-815 CD spectrophotometer (Jasco Analytical Instruments, Easton, MD) in a 0.2 mm path-length cylindrical quartz cuvette (Starna Cells Inc., Atascadero, CA).

Once the scan in water was completed, to the other half of the solution, 75 μ L of NaCl of the appropriate concentrations was added to bring the total concentration in the tubes to 10, 20, 50, 100, or 300 mM NaCl and pipetted to mix. Immediately after addition of NaCl, the BAPC solution CD spectrum was obtained. Once this scan was completed, the sample was left in the cuvette and scanned again after 90 minutes.

After the 90-minute scan was completed, the BAPC in NaCl solution was transferred to a Amicon Ultra-0.5 mL centrifugal cellulose filters with 30 kDa molecular weight cut-off (EMD Millipore, Billerica, MA) and centrifuged at 14000 x g for 5 minutes. This solution was washed with distilled, deionized water once and centrifuged again. The filter was then inverted into a clean tube and centrifuged at 2000 x g for 5 minutes to recover the BAPCs. The BAPC solution was resuspended in 150 μ L water and the absorbance of this solution was also taken at 257.5 nm as described above in order to determine the concentration. This was then put back into the CD cuvette and the spectrum was again scanned as above from 260-190 nm initially after adding the distilled, deionized water to the BAPCs and after 30 minutes.

The CD data was obtained in mdeg values, an average of 5 scans was used, and a blank of either water or the appropriate NaCl solution concentration was subtracted from the raw sample spectra. The spectra were smoothed using a Savitsky–Golay filter within the Spectra Analysis software (Jasco Inc., Easton, MD). Mean residue ellipticity was calculated using this equation:

$$\text{Mean Residue Ellipticity} = \Theta / (n \times c \times l)$$

$$\Theta = \text{CD measurement value in mdeg}$$

n = number of peptide bonds in h_5 and h_9

C = Concentration (M)

l = cuvette path length in cm

Permeability of pH Variations in 5(6)Carboxyfluorescein-containing BAPCs

Initial studies of the permeability of the BAPC bilayer began with an examination of the permeability of the bilayer to hydronium and hydroxide ions. In order to do this, we took advantage of the pH-induced fluorescence changes of 5(6)Carboxyfluorescein dye. This dye alone in solution showed significant changes as the pH was examined from very acidic to basic (**Figure 2.1 Panel A**). As the pH increased from 2 to 9, the fluorescence of the dye solution also increased about 60 absorbance units between each pH change.

When the BAPCs were prepared with encapsulated 5(6)Carboxyfluorescein, the same trend that was seen with the dye in solution was seen with the encapsulated dye (**Figure 2.1 Panel B**). This shows that hydronium and hydroxide ions move rapidly and readily through the BAPC bilayer. This early data shows that we have a membrane that can allow water to pass freely through and may even allow other small molecules.

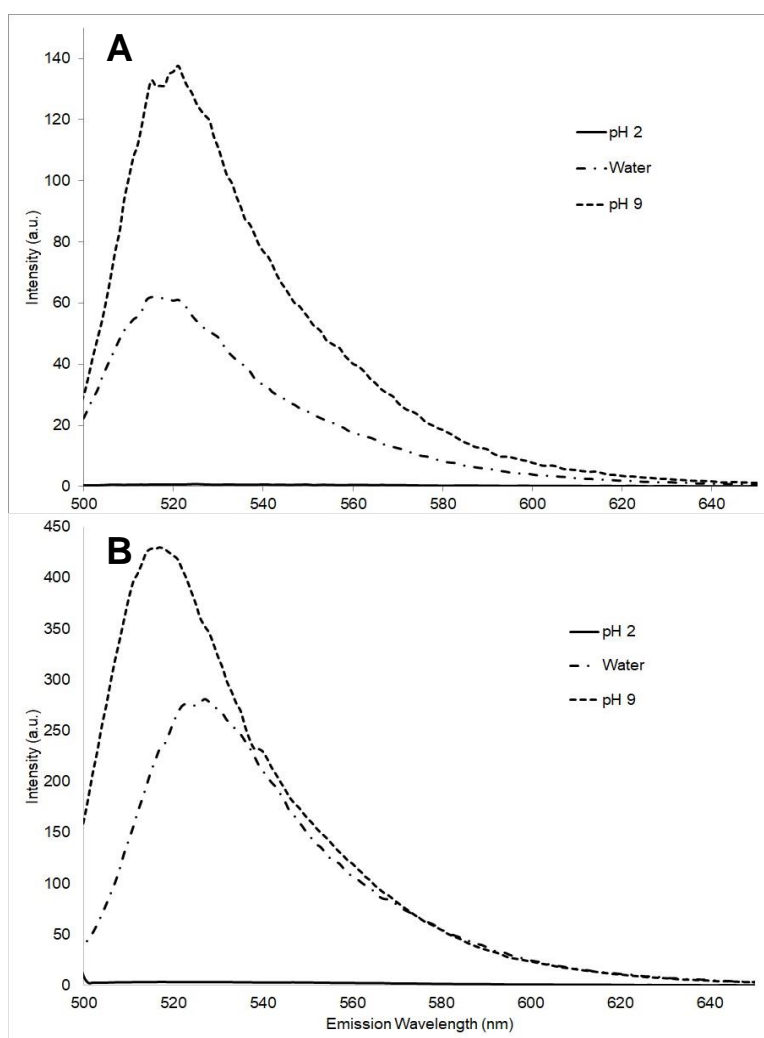


Figure 2.1 – Effects of pH on 5(6)Carboxyfluorescein in Solution and BAPCs

Panel A – 37.5 μ M 5(6)Carboxyfluorescein dissolved in solution listed.

Panel B – BAPCs containing 1.5 mM 5(6)Carboxyfluorescein in water then moved to solution listed. Dashed line shows data in Tris Buffer pH 9, dash-dot line shows data in pure water, and solid line shows data in pH 2 HCl. Graphs show representative data of all runs with $n \geq 3$.

Results of Room Temperature BAPCs in NaCl

Eosin Y Room Temperature BAPC Fluorescence Studies

The purpose of the fluorescence measurements of the Eosin Y-filled BAPCs was to determine the fluorescence change of Eosin Y, which can be then correlated to dilution and size changes within the BAPC populations. Previous work showed that there did not appear to be any ion flow, only water molecules, through the peptide bilayer.⁴⁹ When the water-filled BAPCs' fluorescence were monitored over time in saline solutions, there was an apparent trend that is related to the NaCl concentration (**Figure 2.2**). It can be seen that the fluorescence of the BAPCs in the 10 mM and 20 mM NaCl solutions does not vary much from the initial fluorescence intensity. This suggests that there is very little Eosin Y concentration change and BAPC size fluctuation within these lower concentration saline solutions.

As the NaCl concentrations increases to 50, 100, and 300 mM, it can be seen that there is a marked decrease in the fluorescence intensity with the most intense decrease in fluorescence seen within the first 20 minutes after the BAPCs are placed in the saline solution. This suggests that the Eosin Y within the BAPCs is becoming more concentrated; this is occurring rapidly initially and then the fluorescence remains at about the same level for the remainder of the scans. The decrease in fluorescence intensity occurs in a NaCl concentration-dependent manner, though the 100 mM and 300 mM NaCl curves look similar in both curve and end value. Looking at these curves, it suggests that there is a minimum concentration of NaCl needed in order to drive noticeable water flow out of the BAPCs. It also suggests that the BAPCs can only compress to a certain size, and even with increasing external salt concentration and osmotic pressure, these BAPCs are not able to become any smaller in diameter.

By looking at only the fluorescence values of the 90-minute time points (**Figure 2.3**), the data that the BAPCs only seem to be able to compress to a certain size can be seen more clearly. This data shows that the fluorescence changes that occur from 10 to 50 mM NaCl occur in an almost linear fashion, but at a concentration around 100 mM NaCl, the BAPCs have compressed

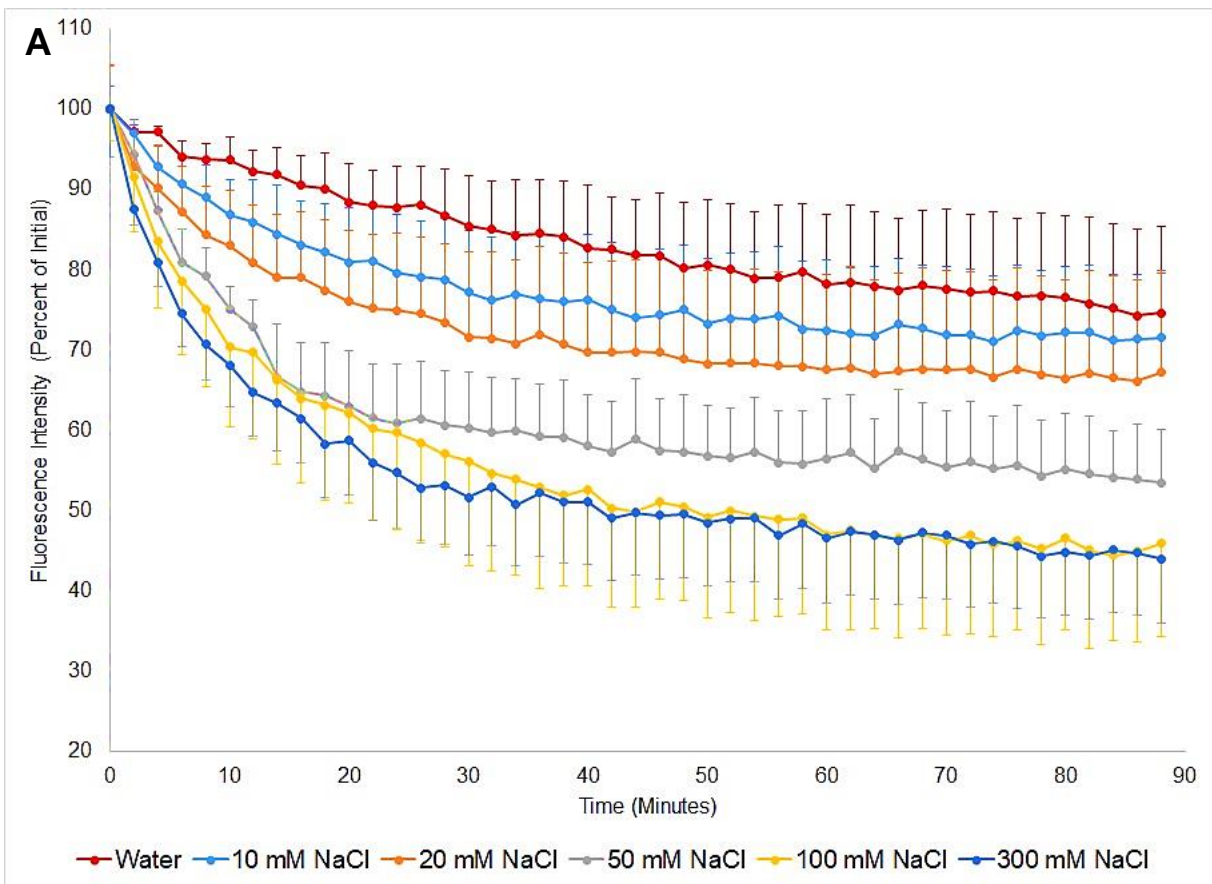
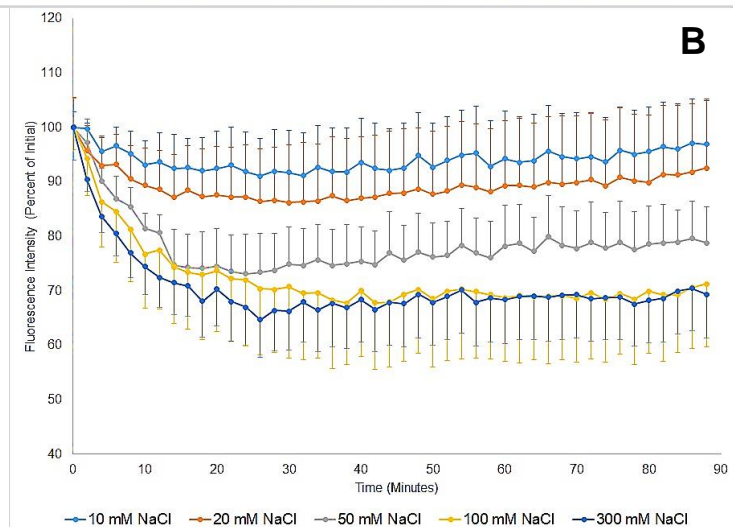


Figure 2.2 – Room temperature BAPCs in NaCl solutions

Shown are the changes in the percent fluorescence intensities. **Panel A** shows the curves including the data from BAPCs in water alone. **Panel B** shows the corrected fluorescence curves when the water values are taken into consideration. Horizontal axis shows the time in minutes from the addition of the saline solution, and the vertical axis has the fluorescence percent values. Error bars show SEM with $n \geq 3$.



as much as they are able to compress, and increasing the saline solution concentration even up to 300 mM does little to further change the BAPC size after 90 minutes.

Once these room temperature BAPCs have had water removed from the internal space and become

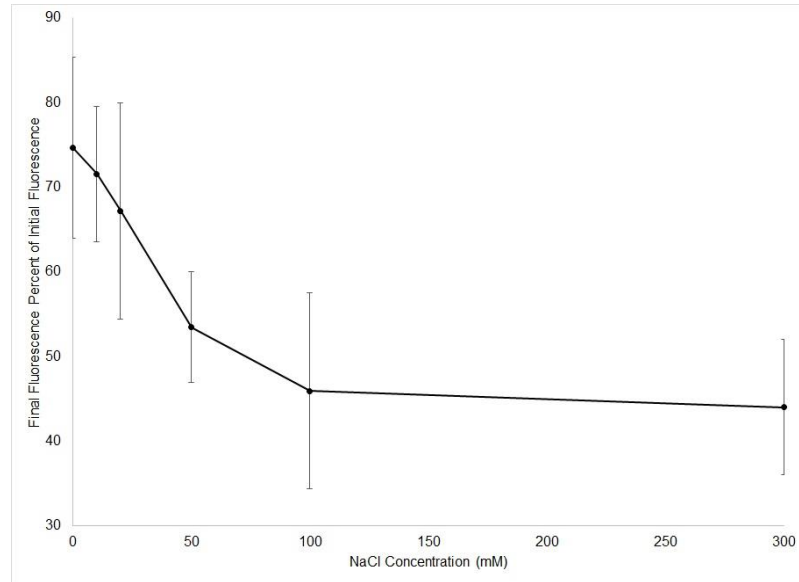


Figure 2.3 – Room temperature BAPC fluorescence values at 90 minutes
Shown are the 90 minute values from **Figure 2.2A** plotted in relation to the concentration of NaCl on the horizontal axis. Error bars show SEM with $n \geq 3$.

more compact, the question then is whether these BAPCs can re-expand when suspended back in a water solution. **Figure 2.4** shows the data of these BAPCs once re-suspended in water after the 90 minutes in a saline solution. When comparing the fluorescence values to those of the final fluorescence, it is seen that there is an increase in fluorescence intensity through all of the concentrations of NaCl. Unlike the graphs seen in **Figure 1.6** that showed a concentration-dependent change in fluorescence, these do not follow the concentration of NaCl from which they were taken. It can be seen here that the BAPCs re-suspended from the 20 mM NaCl solution show the greatest percent increase in fluorescence, which is interesting since they showed little change in fluorescence when put into the NaCl solution. The other BAPCs from the other concentrations of saline solutions also show increasing fluorescence, suggesting that water is moving back into the BAPCs, diluting the Eosin Y within the BAPCs, and therefore, increasing the fluorescence intensity of the Eosin Y.

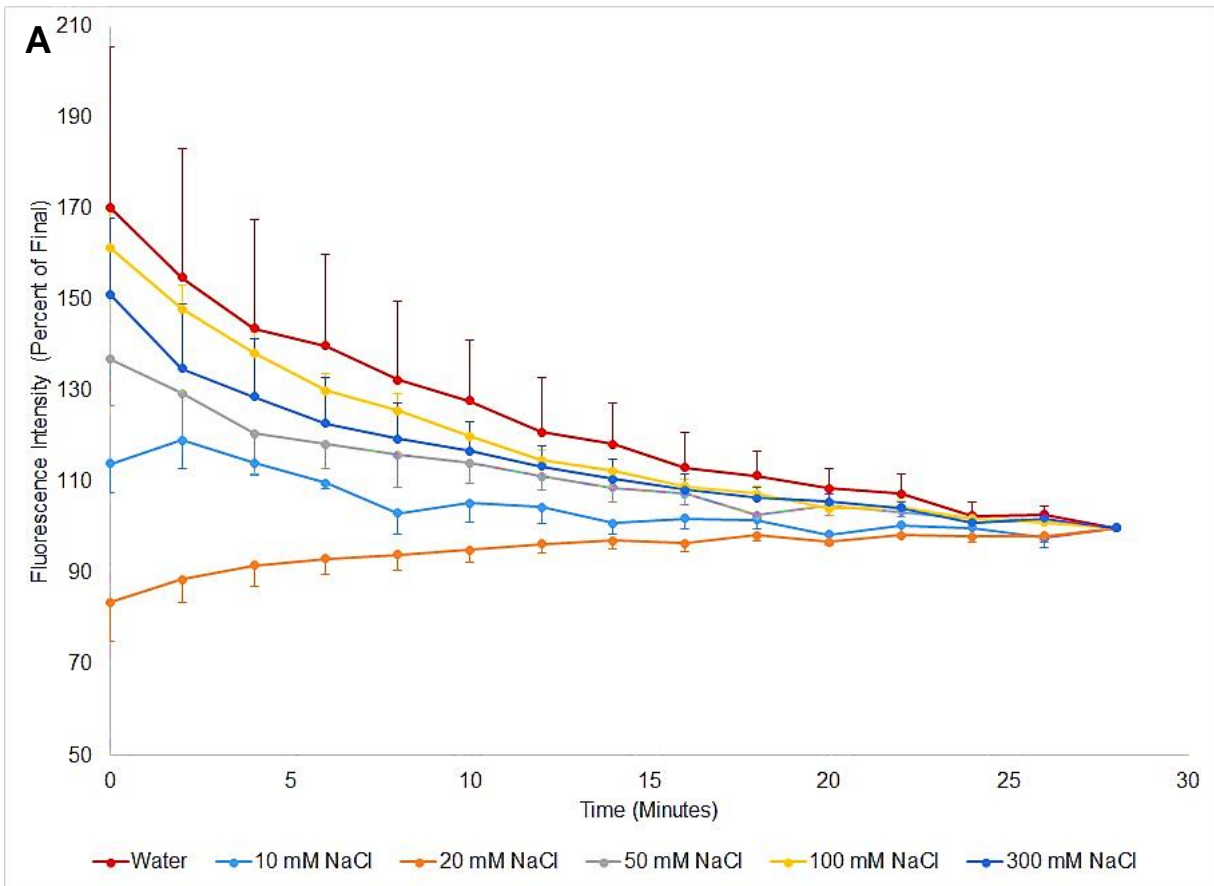
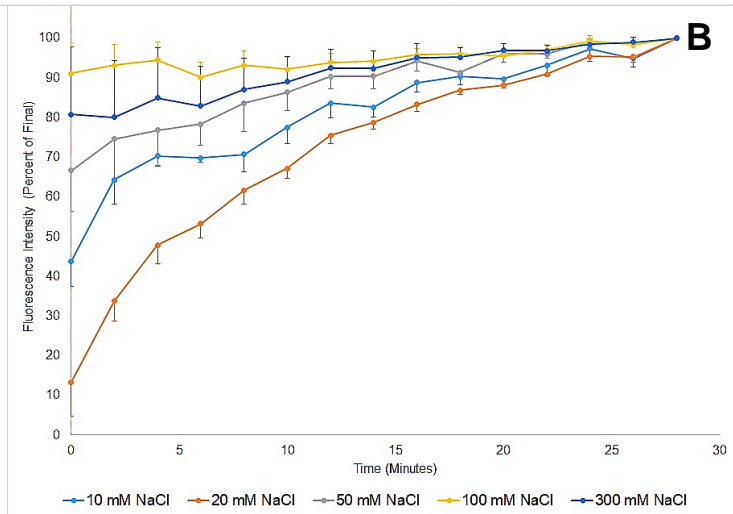


Figure 2.4 – Room temperature BAPCs back to water after NaCl

Shown are the changes in the percent fluorescence intensities in relation to the final fluorescence intensity. **Panel A** shows the curves including the data from BAPCs in water alone.

Panel B shows the corrected fluorescence curves when the water values are taken into consideration. Horizontal axis shows the time in minutes from the resuspension of the filtered BAPCs back into water, and the vertical axis has the fluorescence percent values. Error bars show SEM and $n \geq 3$.



The fluorescence intensity of the initial BAPC scan in water as compared to the final BAPC scan after re-suspension in water can be evaluated to suggest whether the re-suspension of BAPCs allowed the BAPCs to return to their original size. The initial fluorescence divided by the final fluorescence and multiplied by 100 gives us the percent values seen in **Figure 2.5**. The

graph shows that both 10 mM and 20 mM NaCl BAPCs have values less than 100%. A number less than 100% suggests that the initial BAPCs are larger (have more dilute Eosin Y and higher fluorescence) than the final BAPCs that were moved back into water after being in the salt solutions. From this, it seems as though the BAPCs suspended in

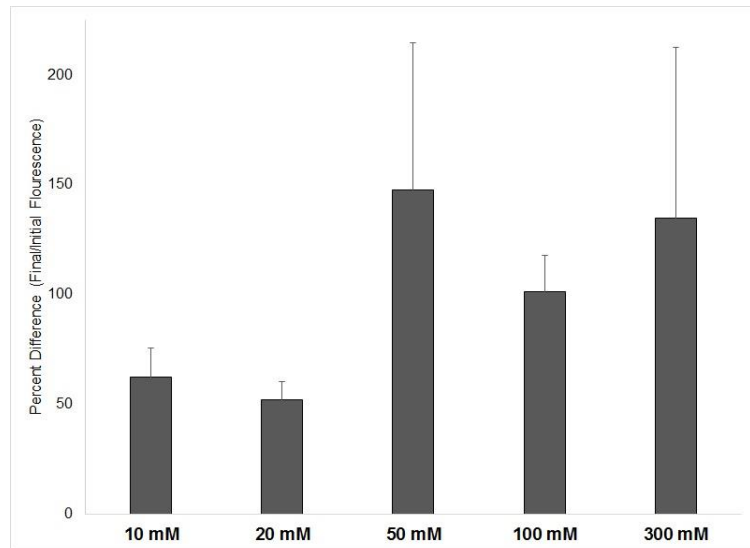


Figure 2.5 – Room temperature BAPCs initial versus final fluorescence
Shown is the percent of the final fluorescence after resuspension in water as compared to the initial fluorescence in water. Values less than 100 suggest that the final BAPC size is smaller than the original size, and values greater than 100 suggest that the final BAPC size is larger than the initial. Error bars are SEM and $n \geq 3$.

these two saline concentrations are unable to return to their original size, even after re-suspension in water and removal of the NaCl. The other saline concentrations show averages that are greater than 100%. Those values larger than 100% suggest that the final size of these BAPCs is larger (have more diluted Eosin Y and a higher fluorescence intensity) than the initial size based on Eosin Y fluorescence. Though those BAPCs that were in 10 and 20 mM NaCl did not seem to show re-expansion to the same size, this highly suggests that the BAPCs are capable of an elastic contraction and expansion to some extent due to osmotic pressure. This expansion and contraction occurs with minimal breakage of the BAPCs, and this can be nearly reversible in regards to the sizes of the BAPCs in the solution.

Room Temperature BAPC Circular Dichroism Studies

The fluorescence studies done on BAPCs in saline solutions showed that the BAPCs have elastic qualities but cannot show how the molecular structure changes due to the saline solution and compression of the BAPC. Previous CD analysis has shown that BAPCs adopt a β -sheet secondary structure upon the addition of NaCl into the solution (data not shown). The earlier work, however, did not show how this secondary structure tendency changed over time, if at all, and whether this secondary structure was reversible when the NaCl was removed from the solution. **Figure 2.6** shows the CD spectra of the BAPCs. All of the initial BAPCs in water show more random coil structure within the secondary structure of the β -sheet as seen by the lessened intensity (more negative) of the values at 195 nm as compared to a pure β -sheet spectrum, which would have a large positive number. Throughout all of the concentrations of NaCl, the CD spectra of the BAPCs shifts to a more pure beta-sheet secondary structure once the NaCl is added to the BAPCs. This can be seen by the strong tendency of the mean residue ellipticity seen at 195 nm to shift to a larger, positive number and the mean residue ellipticity seen at 218 nm to shift to a larger, negative number. It can be seen that there is not much change in the secondary structural characteristics as the BAPCs are allowed to sit in the saline solutions, regardless of the concentration of these solutions. This shows that the effect of the saline solution on secondary structure within the peptides of these room temperature BAPCs happens immediately with little change seen after the initial change occurs.

Once the BAPCs were removed from the saline solutions and re-suspended in water, it can be clearly seen that the CD spectra of the BAPCs does not return to the original spectra, though there are some changes seen in the spectra of the BAPC with and after the addition of NaCl. This suggests that the BAPCs' secondary structures are not just temporarily changed by

the addition of NaCl. The CD spectra seen from BAPCs in 10 mM NaCl suggests that the BAPCs lose some of their β -sheet characteristics once the NaCl is removed and replaced with

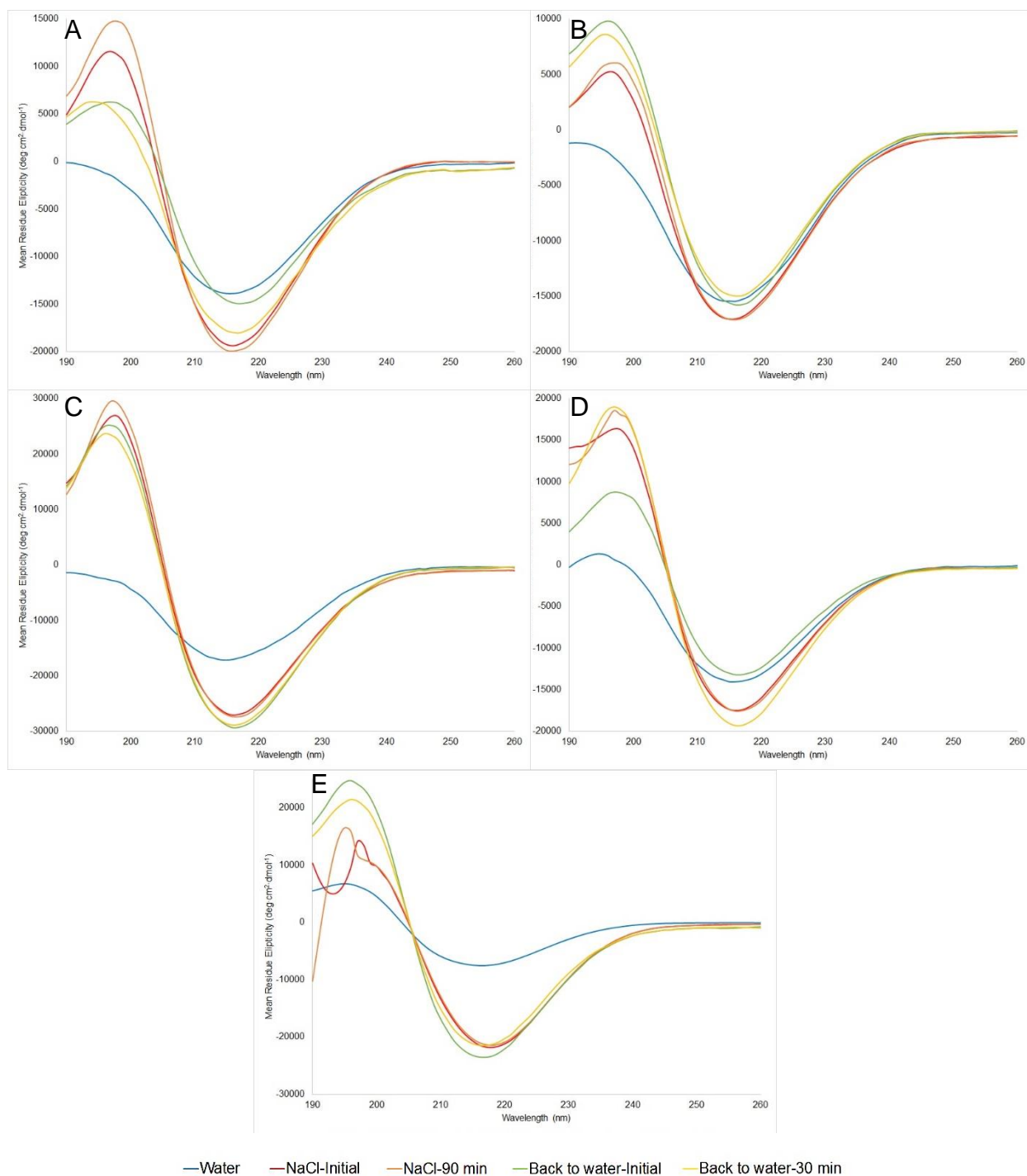


Figure 2.6 – Room temperature BAPC CD spectra

Panels A-E show the CD spectra of BAPCs in NaCl solutions with concentrations as follows: **A – 10 mM NaCl, B – 20 mM NaCl, C – 50 mM NaCl, D – 100 mM NaCl, E – 300 mM NaCl**. The vertical axis shows mean residue ellipticity and the horizontal axis is the wavelength.

pure water. None of the other spectra show this same trend, and BAPCs suspended in 20 mM and 300 mM NaCl even show more β -sheet characteristics in the CD spectra once the NaCl is replaced with water. This data shows that once NaCl has been in the solution, especially in concentrations greater than or equal to 20 mM, the BAPC's secondary structure change is essentially permanent. These structural changes cannot be reversed by removing almost all of the NaCl from the BAPCs, suggesting that the salt drives some kind of reorganization effect within the peptides of the BAPCs.

Results of Locked BAPCs in NaCl

Eosin Y Locked BAPC Fluorescence Studies

As discussed previously, the locked conformation BAPCs are BAPCs that have been made at room temperature and moved to 4°C and back to room temperature. These BAPCs have

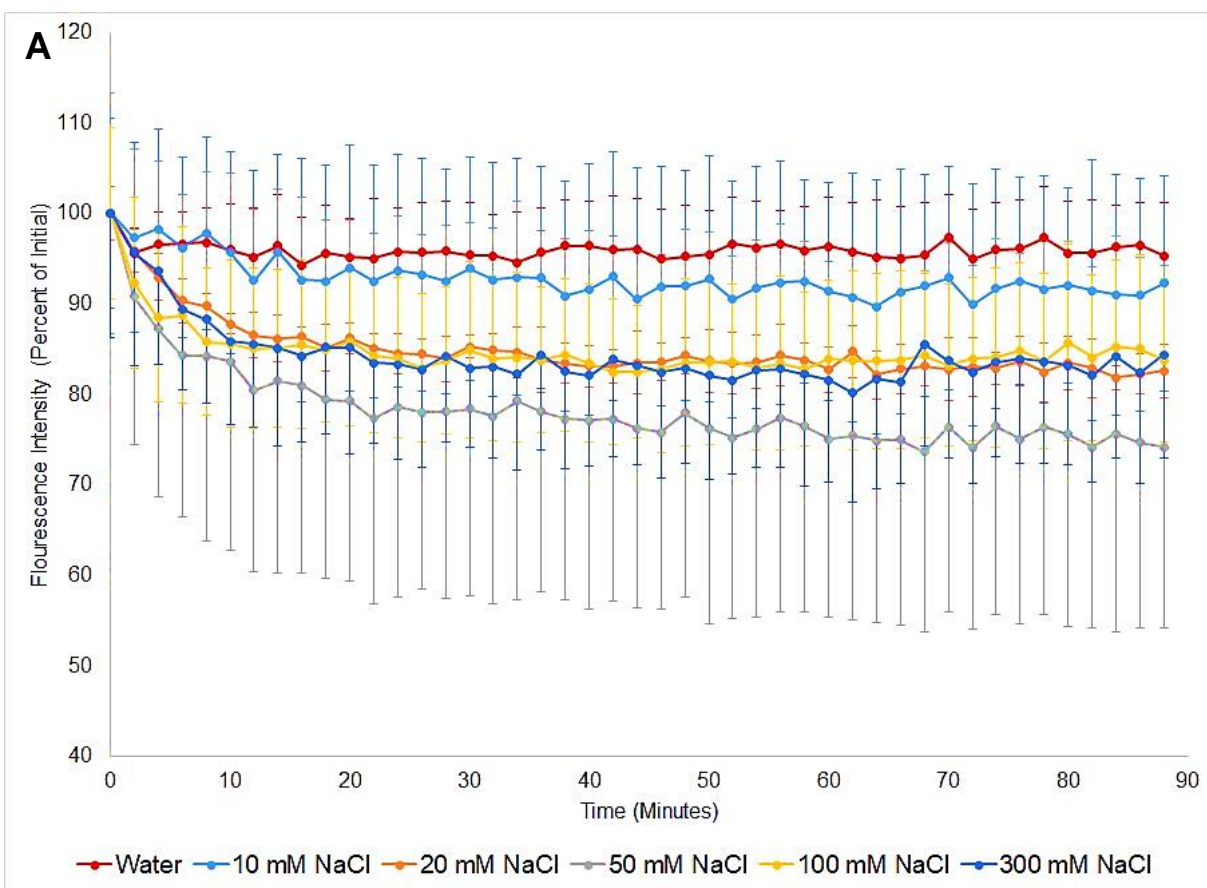
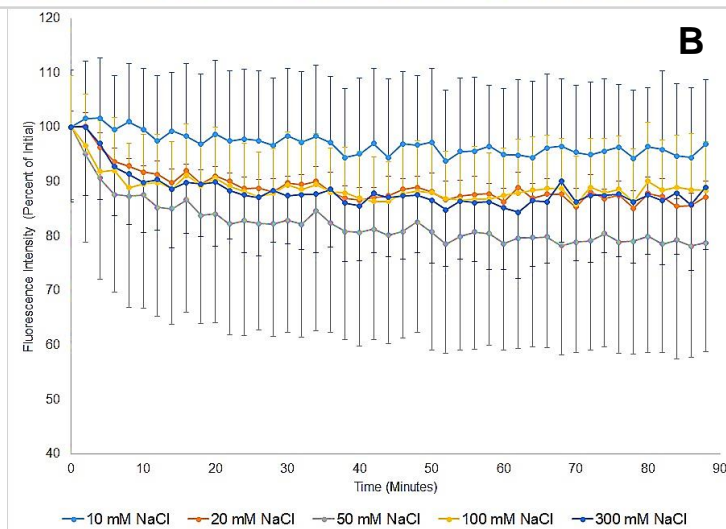


Figure 2.7 - Locked BAPCs in NaCl Solutions

These plots show the changes in the percent fluorescence intensities. **Panel A** shows the curves including the data from BAPCs in water alone. **Panel B** shows the corrected fluorescence curves when the water values are taken into consideration. Horizontal axis shows the time in minutes after the addition of the saline solution, and the vertical axis has the fluorescence percent values as compared to the initial fluorescence value. Error bars show SEM with $n \geq 3$.



unique properties and show promising results for nucleic acid delivery and other potential applications. Due to the potential that these BAPCs have experimentally and therapeutically, it is more important to understand how different conditions, especially those conditions that a BAPC would encounter *in vivo*, change the sizes and affect the BAPCs overall. Using Eosin Y as a gauge for the internal concentration, once again, water flow into and out of the BAPCs can be monitored by measuring changes in the fluorescence intensity.

When locked conformation BAPCs were put into increasing salt concentrations, there was little change seen in the fluorescence values over the 90 minutes during which the scans were done (**Figure 2.7**). In a concentration-dependent manner, the BAPCs within the 10 mM NaCl solution do not have much change in fluorescence values, and the 20 and 50 mM NaCl solutions show

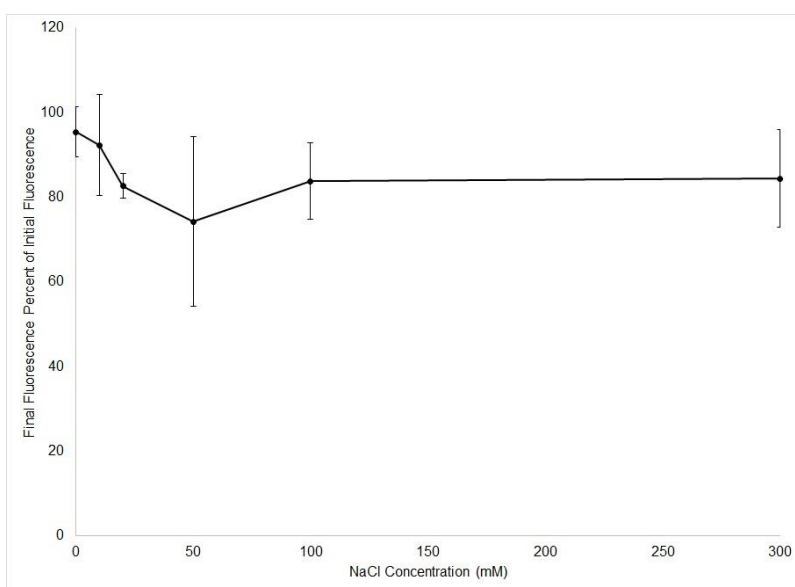


Figure 2.8 – Locked BAPC fluorescence values at 90 minutes
Shown is the data from the final time point in **Figure 2.7A** plotted in relation to NaCl concentration on the horizontal axis. Error bars show SEM with $n \geq 3$.

a slight decrease in fluorescence over the course of the 90 minute scans. This decrease in fluorescence suggests that the Eosin concentration within the BAPCs is increasing as water is moving out. The fluorescence values for the BAPCs within the 100 and 300 mM NaCl solutions do not continue to decrease as expected, though. They follow a curve that is nearly identical to the curve seen for the BAPCs in the 20 mM NaCl. This seems to suggest that there is no more water flow out of the BAPCs suspended in 100 or 300 mM NaCl than there is from those BAPCs

in 20 mM NaCl despite being in about a 10 fold higher salt concentration. The majority of this fluorescence change occurs in the first 20 minutes, much like we saw in the room temperature BAPCs.

These total percent fluorescence changes can more clearly be seen by visualizing only the

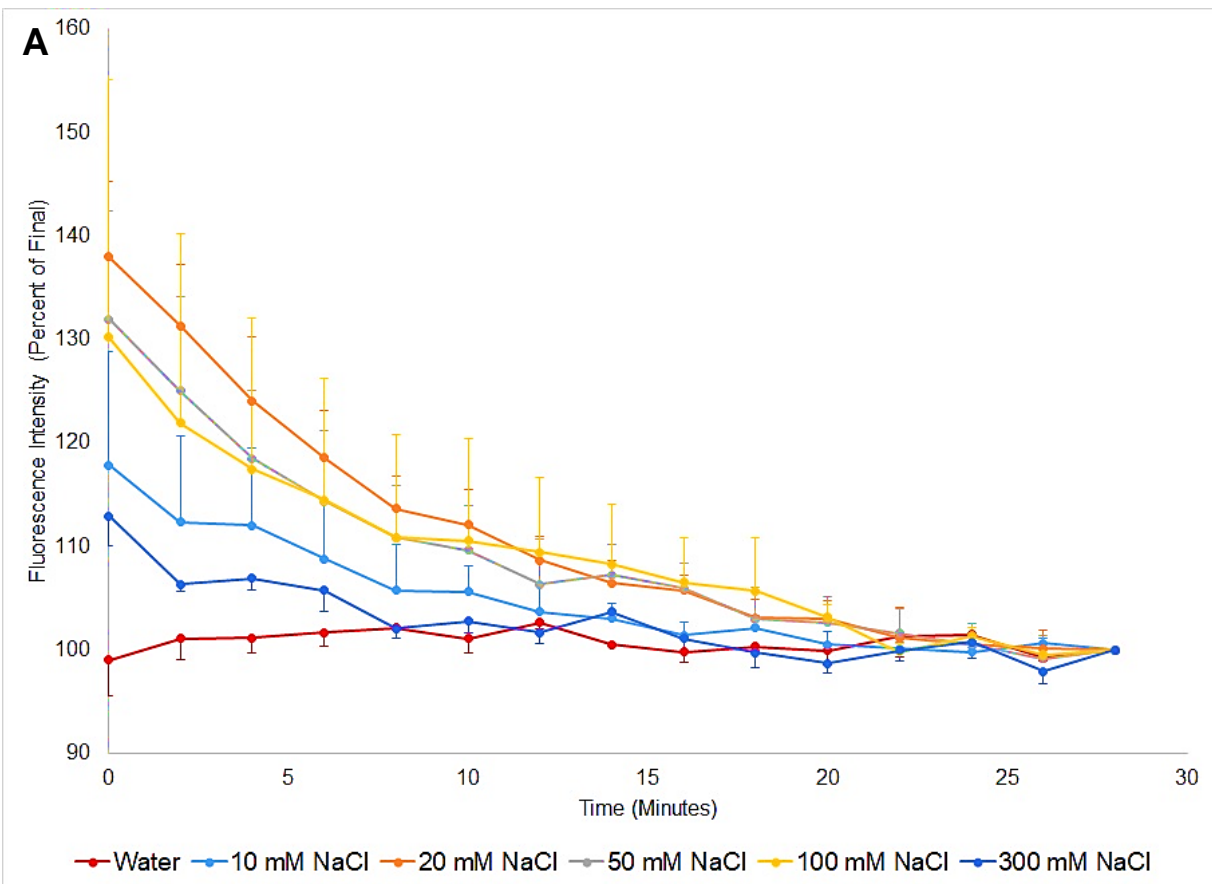
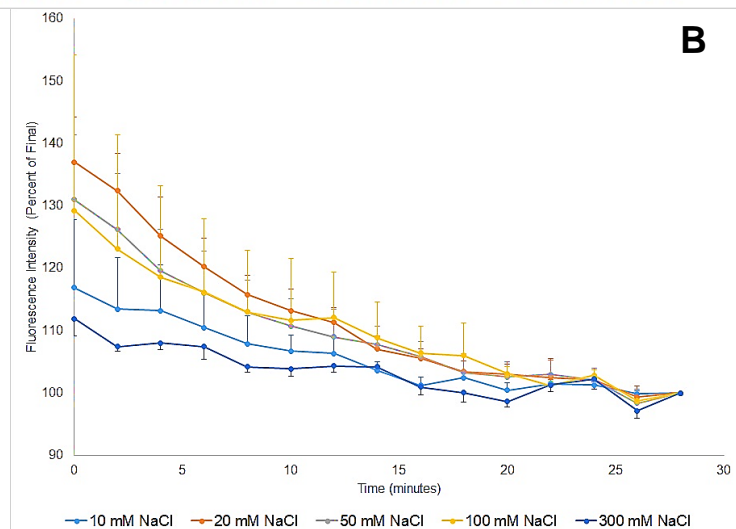


Figure 2.9 – Locked BAPCs back to water after NaCl

These plots show the changes in the percent fluorescence intensities in relation to the final fluorescence intensity once the BAPCs are returned to water. **Panel A** shows the curves including the data from BAPCs in water alone.

Panel B shows the corrected fluorescence curves when the water values are taken into consideration. Horizontal axis shows the time in minutes from the resuspension of the BAPCs back into water, and the vertical axis has the fluorescence percent values. Error bars show SEM and $n \geq 3$.



final percent values after the 90 minutes of scanning were completed (**Figure 2.8**). The BAPCs within the 10 mM NaCl solution remain close to their original fluorescence throughout the 90 minutes, and final fluorescence of the BAPCs within 20 and 50

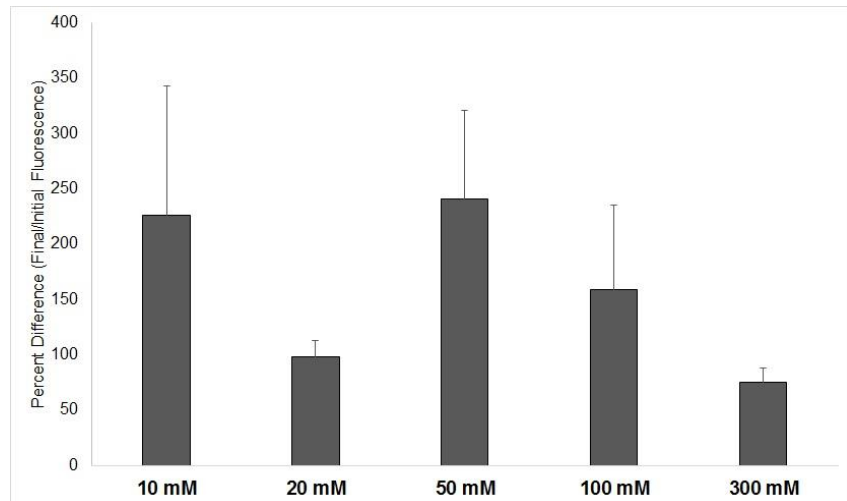


Figure 2.10 – Locked BAPCs initial versus final fluorescence

Data shows the percent of the final fluorescence of BAPCs resuspended in water as compared to the initial fluorescence in water. Values less than 100 suggest that the final BAPC size is smaller than the original size, and values greater than 100 suggest that the final BAPC size is larger than the initial. Error bars are SEM and $n \geq 3$.

mM NaCl decreases in an almost linear fashion in a concentration-dependent manner with the BAPCs in 50 mM NaCl being at about 85% their original fluorescence. The NaCl concentration-dependent trend does not continue for the 100 and 300 mM NaCl solutions. Instead, they show a final fluorescence value that is about 95% of the original value, which is quite similar to that seen for those in 20 mM NaCl solution BAPCs.

When these same locked BAPCs were transferred back into pure distilled, deionized water, the fluorescence effects were quite interesting. Unlike previously seen with the room temperature BAPCS, these locked BAPCs have a continued decrease in fluorescence even after transfer back to water. It can be seen that it is up to a 40% change in fluorescence as compared to the final fluorescence (**Figure 2.9**). Based on the known trends of Eosin Y fluorescence, this suggests that the BAPCs are continuing to move water out of the internal compartment of the BAPC and shrink in size, further concentrating the Eosin Y located inside of the BAPC. This adds to the data showing that these locked BAPCs have unique properties that are not well understood at all times.

This previous data in **Figure 2.9** is somewhat contradicted by taking the initial versus the final fluorescence of the BAPCs in water. It is clearly seen in **Figure 2.10** that the values of 10, 50, and 100 mM NaCl lie at or above 100%, suggesting that the final size of the BAPCs exceeds the initial size. Though this is not fully supported by the data reported in **Figure 2.9**, it also suggests that the locked BAPCs, much like the room temperature BAPCs previously discussed, are flexible and have a dynamic bilayer system that allows for expansion and contraction. Unlike the room temperature BAPCs, locked BAPCs seem to have a greater tendency to remain at or return to at least their initial size even after being in a saline solution.

Locked BAPC Circular Dichroism Studies

Previously published work, as discussed earlier, has shown a difference in the secondary structure of BAPCs that have been taken to 4°C. Even when these BAPCs are then brought back to 25°C (like the locked BAPCs), they still retain some of the random coil structural characteristics of those BAPCs seen at 4°C. This can be clearly seen in the circular dichroism data in **Figure 2.11**. The initial curves of the BAPCs in water show a more negative number at 195 nm as compared to those initial curves of the room temperature BAPCs (**Figure 2.6**). This negative number at this wavelength corresponds to random coil secondary structure. There is still a large negative number at 218 nm which is associated with the β -sheet secondary structure.

Even with the random coil characteristics seen in the locked BAPCs prior to the addition of NaCl, BAPCs in a solution of NaCl in all of the concentrations tested show a strong β -sheet signal with mean residue ellipticity being a large, negative number at 218 nm coupled with a large, positive number at 195 nm. The presence of these β -sheet characteristics seems to increase with the concentration of NaCl, but even the 10 mM NaCl spectra show a definite and noticeable shift toward β -sheet secondary structure. As the BAPCs sit in these saline solutions, there is also minimal change in the structural spectra. This shows that most of the changes that occur in the secondary structure occur upon immediate contact with the ions. Prolonged contact with a solution containing NaCl does not seem to change the structural arrangement much.

This β -sheet structure remains even after the salt is removed in all of the samples tested, and none of these BAPCs return to their original secondary structural spectrum. In the BAPCs within the 10, 20, and 100 mM NaCl, the β -sheet spectral characteristics actually became more pronounced when the NaCl was removed. Even those these locked BAPCs seem to have less elasticity or change as seen in the Eosin Y studies, their structure seems to change readily and

rapidly in the presence of NaCl in the surrounding solution. These locked BAPCs also resist many other changes as previously discussed from earlier publications, but they are not resistant to the semi-permanent or permanent changes from the addition of external NaCl.

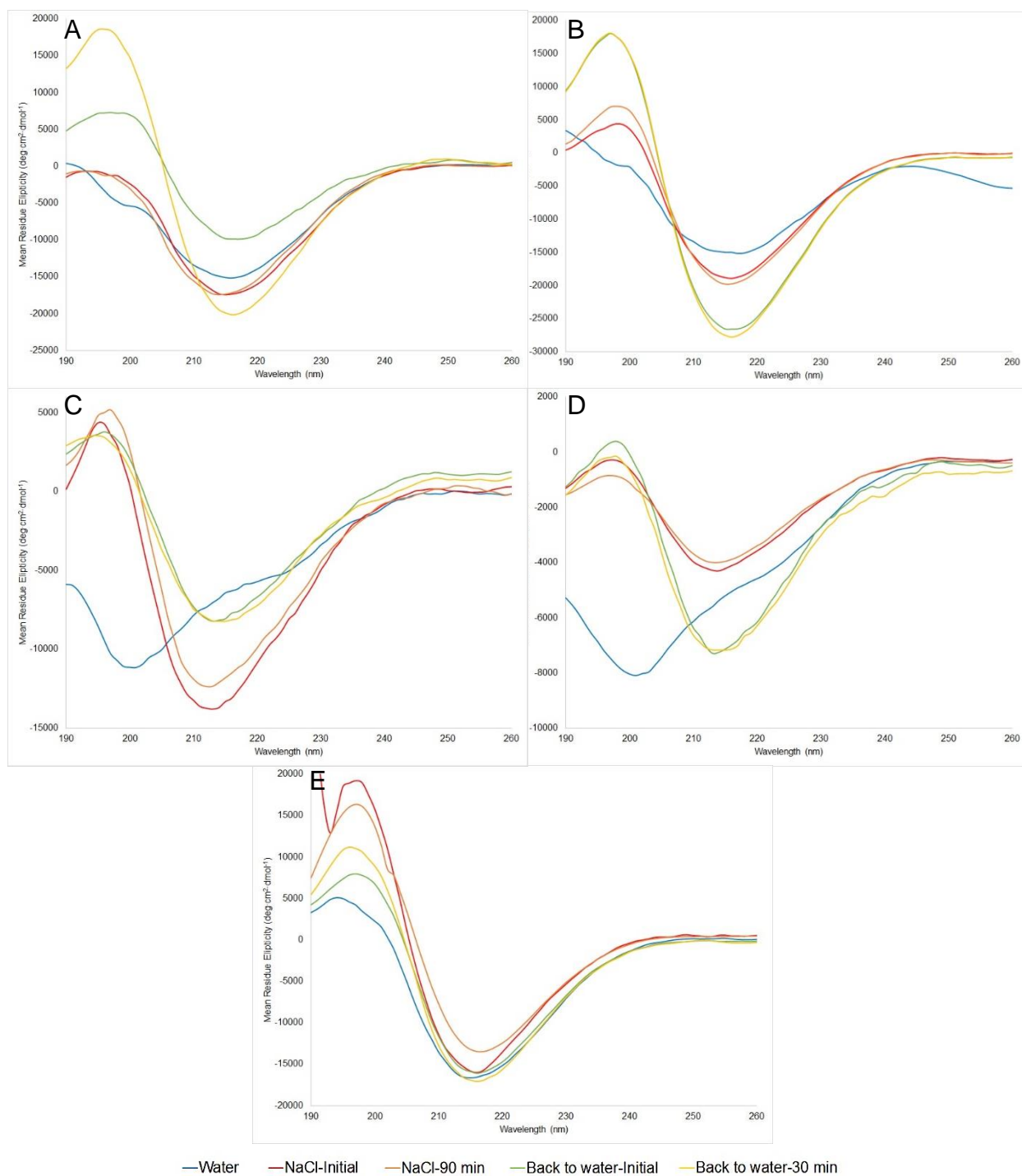


Figure 2.11 – Locked BAPC CD spectra

Shown in panels A-E are the CD spectra of BAPCs in NaCl solutions in the panels as follows: **A – 10 mM NaCl, B – 20 mM NaCl, C – 50 mM NaCl, D – 100 mM NaCl, E – 300 mM NaCl.** The vertical axis shows mean residue ellipticity and the horizontal axis is the wavelength.

Chapter 3 – Discussion and Future Work

Discussion

By looking at the changes that occur with the apparent sizes of the room temperature versus locked BAPCs, it looks as though the locked BAPCs do not have the same ability to shrink and swell as the room temperature BAPCs. The room temperature BAPCs seem to decrease in size in relation to the concentration of the saline solution, but the locked BAPCs do not decrease to the same extent

when moved to higher salt concentrations (**Figure 3.1**).

Previous work has shown that the locked BAPCs are

structurally and

characteristically distinct from

the room temperature BAPCs.

This data presented here agrees

with that. The rearrangement of

the peptides within the BAPC

during the temperature shifts that produce the locked BAPC also modifies the elasticity of the peptide bilayer.

When the BAPCs are returned to water after being in saline solutions, the room temperature BAPCs show a predictable increase in the fluorescence, suggesting that water is moving back into the BAPCs as expected (**Figure 2.4**, **Figure 2.9**). Oddly, this same trend is not seen in the locked BAPCs. Though the locked BAPCs show a change when moved back into a

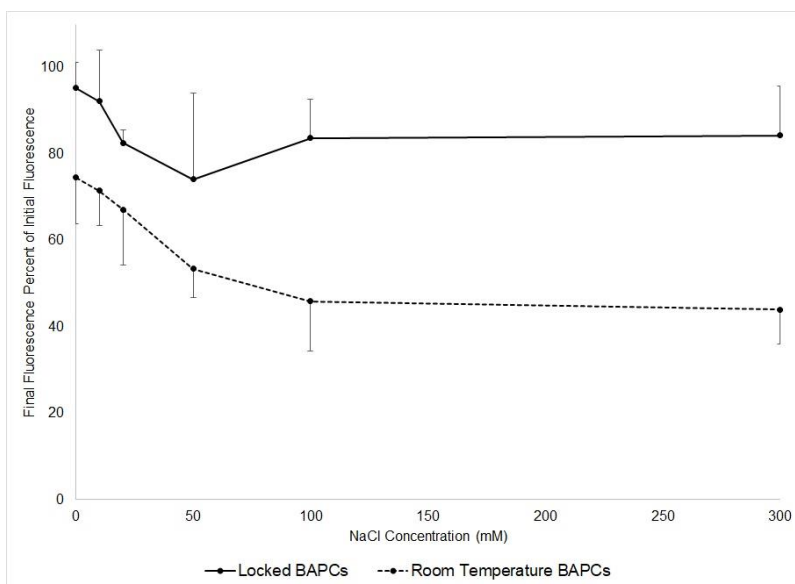


Figure 3.1 - Room Temperature and Locked BAPCs Final Fluorescence
Shown is the combined data from **Figure 2.3** and **Figure 2.8**. The data from the locked BAPCs is shown in a solid line and the data from the room temperature BAPCs is shown in a dashed line. Error bars show SEM with $n \geq 3$.

water solution, it is not the fluorescence direction expected (**Figure 2.9**). Comparing the actual beginning and ending fluorescence values in water in both locked and room temperature BAPCs do show commonalities. Room temperature and locked BAPCs both showed that they were able to reach the same, if not higher, fluorescence values after being moved back into water (**Figure 2.5, Figure 2.10**). This raw fluorescence data shows that the BAPCs have the ability to re-expand to greater than their original size, depending on the saline concentration. This suggests that the temperature-induced changes that occur to make these locked BAPCs unique from the room temperature BAPCs also modifies their compressibility from the osmotic pressure of the saline solutions and makes them have less of a tendency to decrease in size than those BAPCs formed at room temperature, even when in concentrated saline solutions. This work done with Eosin Y BAPC fluorescence seems to agree with previously published data and molecular modeling.

It does not seem as though a charged ion, such as sodium or chloride in solution, can readily cross the BAPC bilayer, much like is seen with the phospholipids of the cell membrane. These unique properties of strength, flexibility, and elasticity along with the ability to selectively exclude a small molecule like an ion but not water make this peptide bilayer an interesting option for filtration. With almost 800 million people globally without access to drinking water, improved filtration is necessary to ensure availability to clean, fresh water for everyone now and in the future.^{50,51} One method that is being investigated is the purification of salt water and brackish water to drinking water. Typically, in order to desalinate sea water, a reverse osmosis (RO) procedure or a traditional distillation procedure is used. These techniques typically use a great deal of energy to remove ions and contaminants from the water.⁵² The membranes that are used for RO can also be adversely effected or ruined by the pH levels or levels of certain ions,

like chloride, in the water they are purifying. In contrast, the BAPC membrane seems to be more robust and does not seem to be affected by pH changes or any of the ions that it has been exposed to.⁵³

Forward osmosis (FO) has become more popular in recent years due to the smaller amount of energy used and the use of osmotic pressure to pull water through a membrane.⁵⁴ This technology is especially important in areas where there is not sufficient power to run desalinization via RO. In these cases, FO stands to be a promising technology to allow access to drinking water.⁵⁴ The use of FO membranes has been shown to be very efficient in removing many salts and organic compounds, but it has been difficult to make or find other selectively permeable membranes to remove small ions, molecules or organic compounds.⁵⁵

The use of peptides and other polymers have begun to be investigated for use in filtration, along with the use of nanocapsules as an option for use in FO technology.^{52,50,54} Because of their chemical synthesis and availability of attachment sites for other molecules, these peptide surfaces can be easily modified to allow for decreased fouling and unwanted attachment to the filter layer.⁵⁶ The hydrophilic residues already on the external portion of the membrane would have a lower chance of fouling from organic compounds. This is due to the hydrogen bonding between the water and the filter surface which prevents adsorption between membrane and organic compounds.⁵⁷ The peptides that form the bilayer itself are very stable and would be straightforward to scale up to make an appropriately sized bilayer for filtration.⁵³ A planar bilayer that mimics the already known bilayer seen in this nanocapsule could be developed from these peptide sequences. There is potential in the future that this bilayer may prevent some of these drawbacks currently seen with FO.

Another option for the BAPCs would be the concentration or purification of other compounds. One type of compound of great interest to purify is pharmaceuticals. Many of the therapeutic agents are pH, temperature, or pressure labile so there aren't many options to purify them that would still keep the compound active.⁵⁸ The BAPC bilayer can be used at many different temperatures and pH values without losing efficacy or membrane stability. This peptide bilayer makes a desirable membrane because of its ability to retain salt yet move water and remain resistant to many conditions that would destroy other membrane systems.⁵⁸

As was previously known from earlier CD data, there are temperature-induced changes in the secondary structure of the peptides, and these changes can be seen in the initial curves of each of the data sets. The addition of random coil characteristics can be seen in the locked BAPC spectra (**Figure 2.11**) as compared to the room temperature BAPCs (**Figure 2.6**). Once the BAPCs are added to the saline solutions, the locked and room temperature BAPCs both change irreversibly to more of a β -sheet structure. Surprisingly, whether the BAPCs are locked or room temperature, when they are exposed to NaCl, they both behave the same and seem to become more ordered.

This increase in order of the peptide secondary structure seems to show that the NaCl ions behave as a kosmotrope, or an order-inducer, which is consistent with previously published data about these ions.^{59,60} It could be that the charges of the ions decrease the repulsion of the positively charged head groups of the lysine residues.⁵⁹ It could also be that both sodium and chloride have a relatively strong interaction with water. Having this strong interaction with water is another property that causes them to behave as a kosmotrope.⁶¹ With these ions present in the water at the concentrations used in this work, the polar water molecules are affected, which can change the interaction of the solvent with the residues of the BAPCs. This rearrangement of

water to a more ordered state due to intermolecular hydrogen bonding may also allow for greater expansion and contraction of the water itself. This may lend itself to enhancing the elasticity of the BAPC.⁶⁰ If these ions are present during the self-assembly process of the BAPC, they could increase the hydrophobic interactions between the tails of the peptides. This increased aggregation of the tails could also increase order and stability of the BAPC.⁶²

Another potential reason that the BAPCs can contract and change into a more organized structure in the presence of NaCl is the displacement of the TFA salt present on the BAPCs. TFA is present on the peptides from the cleavage solution that liberates the peptide from the resin. Earlier work showed a strong signal from the TFA using ¹⁹F NMR. It is possible to replace the large TFA molecule on the peptide with the smaller chloride ion using HCl.⁶³ It could also be possible that the TFA present on the peptides can also be displaced with moderate to high concentrations of Cl⁻. This less bulky and less hydrophobic molecule acting as a counter-ion on the positive charges of the lysine residues could allow for more contractility, flexibility, and ordering of the BAPC bilayer.

These methods for size approximation and size changes do have their disadvantages and problems. As was discussed previously, **Figure 2.9** and **Figure 2.10** seem to contradict each other somewhat. When the locked BAPCs are moved back into water after being in saline solutions, the fluorescence is expected to increase some as seen with the raw fluorescence values in **Figure 2.10**, but the corrected percent fluorescence continues to decrease (**Figure 2.9**). Unlike the raw data, the decrease in fluorescence suggests that water continues to move out of the BAPCs. This discrepancy brings to light potential issues with only using Eosin Y or Rhodamine 6G as our gauge for size changes.

Future Work

As mentioned in the previous section, further information is needed to ensure that the data obtained from the fluorescence readings accurately describes the behavior of the BAPCs in these saline solutions. One method that has been used with BAPCs in the past is dynamic light scattering (DLS). DLS has the advantage in this experiment because such experiments are done in solution, whether saline or water, and the changes in solution can be monitored as they are with Eosin Y BAPCs.

Because of the physiological relevance of sodium and chloride, these two ions were the first chosen for the initial work done with BAPCs and ions. Depending on the physiological location, the concentration of ions can fluctuate dramatically. It is important to understand how these BAPCs behave when exposed to different ions, both monovalent and divalent, and of different sizes, whether it be the hydrated radius or the radius without the attached water molecules. It is important to understand how changing the anion or cation affects the BAPCs' behavior, and if it is possible to decrease the stability of the peptides through the use of ions.

Publications discussed previously discuss these BAPCs for use as a gene delivery vehicle.^{47,48} When using these as a method for gene delivery, locked BAPCs were used. It has been shown how these locked BAPCs behave in the saline solutions, but it is unknown how having the plasmid around the external surface of the BAPC affects the expansion or contraction of the BAPC. There is the possibility that the DNA may cancel out the positive charges of the lysine residues located on the external face of the BAPC and allow for further contraction within saline solutions. If the positive charges of the phosphates in the DNA backbone do allow for further contraction, it is also necessary to investigate whether this is also true with phosphate in solution. This question goes back to the previous statement about the effect of different ions,

including differences between monovalent and divalent ions. There may also be saline concentrations at which the DNA comes off of the BAPC, and if these are to be used as a gene delivery method, knowing when the DNA can be competed off of the BAPCs by salt in solution is necessary.

A paper recently published also brings to light a few more questions regarding the sizing of the BAPCs.⁶⁴ This work discusses the use of variable h₅ and h₉ ratios to modify the size and transfection of the BAPCs. It is clearly seen that the BAPCs made up purely of h₉ are much smaller than the BAPCs made up purely of h₅; the diameters of these are about 10 nm and 45 nm, respectively. When using both of these as a transfection agent, the smaller BAPCs consisting of pure h₉ proved to be the most efficient in delivering DNA to HEK-293 cells.

This raises a few questions for future work. The BAPCs made up of pure h₉ have a structure that is mainly β -sheet. This is similar to the BAPCs in saline solutions. The BAPCs in saline solutions have shown a propensity to β -sheet structures, which can be suggested that this aids in tighter packing and smaller capsules. With the addition of the osmotic pressure on the BAPCs, they may get smaller than previously seen. The decrease in size may allow the BAPCs to become even more efficient at DNA delivery. It also necessitates looking at the pure h₉ BAPCs in saline solutions. If these are the most relevant BAPCs for future work with these capsules, they also need to be thoroughly investigated in the presence of ions. It begs to question whether these BAPCs can compress anymore and increase their benefits in the world of research and therapeutics.

The work discussed within this paper only begins to scratch the surface of these unique capsules. These BAPCs have the ability to contract, expand, and rearrange the peptides within them, all while remaining intact and stable. Size, stability, and ion effects are all necessary

aspects to understand fully when hoping to use this in the future as a potential therapeutic or delivery vehicle.

References

-
- ¹ Müller, B., & Van de Voorde, M. (Eds.). (2017). *Nanoscience and nanotechnology for human health*. Weinheim, Germany: Wiley-VCH.
- ² Wong, J. K. L., Mohseni, R., Hamidieh, A. A., MacLaren, R. E., Habib, N., & Seifalian, A. M. (2017). Will Nanotechnology Bring New Hope for Gene Delivery? *Trends in Biotechnology*, 35(5), 434–451. <http://doi.org/10.1016/j.tibtech.2016.12.009>
- ³ Mishra, B., Patel, B. B., & Tiwari, S. (2010). Colloidal nanocarriers: a review on formulation technology, types and applications toward targeted drug delivery. *Nanomedicine: Nanotechnology, Biology, and Medicine*, 6(1), 9–24. <http://doi.org/10.1016/j.nano.2009.04.008>
- ⁴ Henderson, L. A. (2016). National Institutes of Health: An Introduction to Nanotechnology Funded Research in Biology and Medicine, Cheng, H. N., Doemeny, L., Geraci, C. L., & Schmidt, D. G. (Eds.) *Nanotechnology: Delivering on the promise* (Volume 1), (59–66). Washington, DC: American Chemical Society.
- ⁵ Mandal, D., Dinda, S., Choudhury, P., & Das, P. K. (2016). Solvent induced morphological evolution of cholesterol based glucose tailored amphiphiles: Transformation from vesicles to nanoribbons. *Langmuir*, 32(38), 9780–9789. <http://doi.org/10.1021/acs.langmuir.6b02165>
- ⁶ Sahoo, S. K., Parveen, S., & Panda, J. J. (2007). The present and future of nanotechnology in human health care. *Nanomedicine: Nanotechnology, Biology, and Medicine*, 3(1), 20–31. <http://doi.org/10.1016/j.nano.2006.11.008>
- ⁷ Ferrari, M. (2005). Cancer nanotechnology: Opportunities and challenges. *Nature Reviews Cancer*, 5(3), 161–171. <http://doi.org/10.1038/nrc1566>
- ⁸ Mo, Z. C., Ren, K., Liu, X., Tang, Z. L., & Yi, G. H. (2016). A high-density lipoprotein-mediated drug delivery system. *Advanced Drug Delivery Reviews*, 106, 132–147. <http://doi.org/10.1016/j.addr.2016.04.030>
- ⁹ Barry, M., Pearce, H., Cross, L., Tatullo, M., & Gaharwar, A. K. (2016). Advances in Nanotechnology for the Treatment of Osteoporosis. *Current Osteoporosis Reports*, 14(3), 87–94. <http://doi.org/10.1007/s11914-016-0306-3>
- ¹⁰ Griffin, B. T., Guo, J., Presas, E., Donovan, M. D., Alonso, M. J., & O'Driscoll, C. M. (2016). Pharmacokinetic, pharmacodynamic and biodistribution following oral administration of nanocarriers containing peptide and protein drugs. *Advanced Drug Delivery Reviews*, 106, 367–380. <http://doi.org/10.1016/j.addr.2016.06.006>

-
- ¹¹ Choi, H. S., Liu, W., Misra, P., Tanaka, E., Zimmer, J. P., Ipe, B. I., Bawendi, M. G., & Frangioni, J. V. (2007). Renal clearance of nanoparticles. *Nat. Biotechnol.*, 25(10), 1165–1170. <http://doi.org/10.1038/nbt1340>.Renal
- ¹² Bayford, R., Rademacher, T., Roitt, I., & Wang, S. X. (2017). Emerging applications of nanotechnology for diagnosis and therapy of disease: A review. *Physiological Measurement*, 38(8), R183–R203. <http://doi.org/10.1088/1361-6579/aa7182>
- ¹³ Niu, Z., Tedesco, E., Benetti, F., Mabondzo, A., Montagner, I. M., Marigo, I., Gonzalez-Touceda, D., Tovar, S., Diéguez, C., Santander-Ortega, M. J., & Alonso, M. J. (2016). Rational design of polyarginine nanocapsules intended to help peptides overcoming intestinal barriers. *Journal of Controlled Release*. <http://doi.org/10.1016/j.jconrel.2017.02.024>
- ¹⁴ Herrmann, I. K., & Rösslein, M. (2016). Personalized medicine: The enabling role of nanotechnology. *Nanomedicine*, 11(1), 1–3. <http://doi.org/10.2217/nnm.15.152>
- ¹⁵ Azzawi, M., Seifalian, A., & Ahmed, W. (2016). Nanotechnology for the diagnosis and treatment of diseases. *Nanomedicine*, 11(16), 2025–2027. <http://doi.org/10.2217/nnm-2016-8000>
- ¹⁶ Lollo, G., Gonzalez-Paredes, A., Garcia-Fuentes, M., Calvo, P., Torres, D., & Alonso, M. J. (2017). Polyarginine nanocapsules as a potential oral peptide delivery carrier. *Journal of Pharmaceutical Sciences*, 106(2), 611–618. <http://doi.org/10.1016/j.xphs.2016.09.029>
- ¹⁷ Cui, H., & Chen, X. (2017). Peptides and peptide conjugates in medicine. *Advanced Drug Delivery Reviews*, 110–111, 1–2. <http://doi.org/10.1016/j.addr.2017.04.004>
- ¹⁸ Acar, H., Srivastava, S., Chung, E. J., Schnorenberg, M. R., Barrett, J. C., LaBelle, J. L., & Tirrell, M. (2017). Self-assembling peptide-based building blocks in medical applications. *Advanced Drug Delivery Reviews*, 110–111, 65–79. <http://doi.org/10.1016/j.addr.2016.08.006>
- ¹⁹ Sun, X., Li, Y., Liu, T., Li, Z., Zhang, X., & Chen, X. (2017). Peptide-based imaging agents for cancer detection. *Advanced Drug Delivery Reviews*, 110–111, 38–51. <http://doi.org/10.1016/j.addr.2016.06.007>
- ²⁰ Sapsford, K. E., Algar, W. R., Berti, L., Gemmill, K. B., Casey, B. J., Oh, E., Stewart, M. H., & Medintz, I. L. (2013). Functionalizing nanoparticles with biological molecules: Developing chemistries that facilitate nanotechnology. *Chemical Reviews*, 113(3), 1904–2074. <http://doi.org/10.1021/cr300143v>
- ²¹ Eskandari, S., Guerin, T., Toth, I., & Stephenson, R. J. (2017). Recent advances in self-assembled peptides: Implications for targeted drug delivery and vaccine engineering.

Advanced Drug Delivery Reviews, 110–111, 169–187.
<http://doi.org/10.1016/j.addr.2016.06.013>

- ²² Ruoslahti, E. (2017). Tumor penetrating peptides for improved drug delivery. *Advanced Drug Delivery Reviews*, 110–111, 3–12. <http://doi.org/10.1016/j.addr.2016.03.008>
- ²³ Kuang, H., Ku, S. H., & Kokkoli, E. (2017). The design of peptide-amphiphiles as functional ligands for liposomal anticancer drug and gene delivery. *Advanced Drug Delivery Reviews*, 110–111, 80–101. <http://doi.org/10.1016/j.addr.2016.08.005>
- ²⁴ Brezaniouva, I., Hruby, M., Kralova, J., Kral, V., Cernochova, Z., Cernoch, P., Slouf, M., Kredatusova, J., & Stepanek, P. (2016). Temoporphin-loaded 1-tetradecanol-based thermoresponsive solid lipid nanoparticles for photodynamic therapy. *Journal of Controlled Release*, 241, 34–44. <http://doi.org/10.1016/j.jconrel.2016.09.009>
- ²⁵ Peyret, A., Ibarboure, E., Pippa, N., & Lecommandoux, S. (2017). Liposomes in polymersomes: Multicompartment system with temperature-triggered release, *Langmuir*, 33, 7079–7085. <http://doi.org/10.1021/acs.langmuir.7b00655>
- ²⁶ Randles, E. G., & Bergethon, P. R. (2013). A photodependent switch of liposome stability and permeability. *Langmuir*, 29(5), 1490–1497. <http://doi.org/10.1021/la303526k>
- ²⁷ Blanco, E., Shen, H., & Ferrari, M. (2015). Principles of nanoparticle design for overcoming biological barriers to drug delivery. *Nature Biotechnology*, 33(9), 941–951. <http://doi.org/10.1038/nbt.3330>
- ²⁸ Gharpure, K. M., Wu, S. Y., Li, C., Lopez-Berestein, G., & Sood, A. K. (2015). Nanotechnology: Future of Oncotherapy. *Clinical Cancer Research*, 21(14), 3121–3130. <http://doi.org/10.1158/1078-0432.CCR-14-1189>
- ²⁹ Le Garrec, D., Ranger, M., & Leroux, J.-C. (2004). Micelles in anticancer drug delivery. *American Journal of Drug Delivery*, 2(1), 15–42. <http://doi.org/10.2165/00137696-200402010-00002>
- ³⁰ Niu, D., Li, Y., & Shi, J. (2017). Silica/organosilica cross-linked block copolymer micelles: A versatile theranostic platform. *Chem. Soc. Rev.*, 46(3), 569–585. <http://doi.org/10.1039/C6CS00495D>
- ³¹ Zuo, Y., Kong, M., Mu, Y., Feng, C., & Chen, X. (2017). Chitosan based nanogels stepwise response to intracellular delivery kinetics for enhanced delivery of doxorubicin. *International Journal of Biological Macromolecules*, 104, 157–164. <http://doi.org/10.1016/j.ijbiomac.2017.06.020>



-
- ³² Liu, R., Li, X., Xiao, W., & Lam, K. S. (2017). Tumor-targeting peptides from combinatorial libraries. *Advanced Drug Delivery Reviews*, 110–111, 13–37. <http://doi.org/10.1016/j.addr.2016.05.009>
- ³³ Rajagopal, K., & Schneider, J. P. (2004). Self-assembling peptides and proteins for nanotechnological applications. *Current Opinion in Structural Biology*, 14(4), 480–486. <http://doi.org/10.1016/j.sbi.2004.06.006>
- ³⁴ Gonzalez-Paredes, A., Torres, D., & Alonso, M. J. (2017). Polyarginine nanocapsules: A versatile nanocarrier with potential in transmucosal drug delivery. *International Journal of Pharmaceutics*. <http://doi.org/10.1016/j.ijpharm.2017.07.001>
- ³⁵ Min, K. I., Yun, G., Jang, Y., Kim, K. R., Ko, Y. H., Jang, H. S., Lee, Y. S., Kim, K., & Kim, D. P. (2016). Covalent self-assembly and one-step photocrosslinking of tyrosine-rich oligopeptides to form diverse nanostructures. *Angewandte Chemie - International Edition*, 128, 7039–7042. <http://doi.org/10.1002/anie.201601675>
- ³⁶ Liu, Y., Liu, C. Y., & Liu, Y. (2011). Investigation on fluorescence quenching of dyes by graphite oxide and graphene. *Applied Surface Science*, 257(13), 5513–5518. <http://doi.org/10.1016/j.apsusc.2010.12.136>
- ³⁷ Wang, Y., Lomakin, A., Kanai, S., Alex, R., Belli, S., Donzelli, M., & Benedek, G. B. (2016). The molecular basis for the prolonged blood circulation of lipidated incretin peptides: Peptide oligomerization or binding to serum albumin? *Journal of Controlled Release*, 241, 25–33. <http://doi.org/10.1016/j.jconrel.2016.08.035>
- ³⁸ Ruttala, H. B., Ramasamy, T., Shin, B. S., Choi, H. G., Yong, C. S., & Kim, J. O. (2017). Layer-by-layer assembly of hierarchical nanoarchitectures to enhance the systemic performance of nanoparticle albumin-bound paclitaxel. *International Journal of Pharmaceutics*, 519(1–2), 11–21. <http://doi.org/10.1016/j.ijpharm.2017.01.011>
- ³⁹ Lehto, T., Ezzat, K., Wood, M. J. A., & Andaloussi, S. EL. (2016). Peptides for nucleic acid delivery. *Advanced Drug Delivery Reviews*, 106(2016), 172–182. <http://doi.org/10.1016/j.addr.2016.06.008>
- ⁴⁰ Englert, C., Trützschler, A. K., Raasch, M., Bus, T., Borchers, P., Mosig, A. S., Traeger, A., & Schubert, U. S. (2016). Crossing the blood-brain barrier: Glutathione-conjugated poly(ethylene imine) for gene delivery. *Journal of Controlled Release*, 241, 1–14. <http://doi.org/10.1016/j.jconrel.2016.08.039>
- ⁴¹ Gudlur, S., Sukthankar, P., Gao, J., Avila, L. A., Hiromasa, Y., Chen, J., Iwamoto, T., & Tomich, J. M. (2012). Peptide nanovesicles formed by the self-assembly of branched amphiphilic peptides. *PLoS ONE*, 7(9). <http://doi.org/10.1371/journal.pone.0045374>

-
- ⁴² Sukthankar, P., Gudlur, S., Avila, L. A., Whitaker, S. K., Katz, B. B., Hiromasa, Y., Gao, J., Thapa, P., Moore, D., Iwamoto, T., Chen, J., & Tomich, J. M. (2013). Branched oligopeptides form nanocapsules with lipid vesicle characteristics. *Langmuir*, 29, 14648–14654. <http://doi.org/10.1021/la403492n>
- ⁴³ Sukthankar, P., Whitaker, S. K., Garcia, M., Herrera, A., Boatwright, M., Prakash, O., & Tomich, J. M. (2015). Thermally induced conformational transitions in nascent branched amphiphilic peptide capsules. *Langmuir*, 31(10), 2946–2955. <http://doi.org/10.1021/la504381y>
- ⁴⁴ Sukthankar, P., Avila, L. A., Whitaker, S. K., Iwamoto, T., Morgenstern, A., Apostolidis, C., Liu, K., Hanzlik, R. P., Dadachova, E., & Tomich, J. M. (2014). Branched amphiphilic peptide capsules: Cellular uptake and retention of encapsulated solutes. *Biochimica et Biophysica Acta - Biomembranes*, 1838(9), 2296–2305. <http://doi.org/10.1016/j.bbamem.2014.02.005>
- ⁴⁵ Richard, I., Thibault, M., De Crescenzo, G., Buschmann, M. D., & Lavertu, M. (2013). Ionization behavior of chitosan and chitosan-DNA polyplexes indicate that chitosan has a similar capability to induce a proton-sponge effect as PEI. *Biomacromolecules*, 14(6), 1732–1740. <http://doi.org/10.1021/bm4000713>
- ⁴⁶ Benjaminsen, R. V., Matthebjerg, M. A., Henriksen, J. R., Moghimi, S. M., & Andresen, T. L. (2012). The possible “proton sponge” effect of polyethylenimine (PEI) does not include change in lysosomal pH. *Molecular Therapy*, 21(1), 149–157. <http://doi.org/10.1038/mt.2012.185>
- ⁴⁷ Avila, L. A., Aps, L. R. M. M., Ploscariu, N., Sukthankar, P., Guo, R., Wilkinson, K. E., Games, P., Szoszkiewicz, R., Alves, R. P. S., Diniz, M. O., Fang, Y., Ferreira, L. C. S. & Tomich, J. M. (2016). Gene delivery and immunomodulatory effects of plasmid DNA associated with branched amphiphilic peptide capsules. *Journal of Controlled Release*, 241, 15–24. <http://doi.org/10.1016/j.jconrel.2016.08.042>
- ⁴⁸ Avila, L. A., Aps, L. R. M. M., Sukthankar, P., Ploscariu, N., Gudlur, S., Šimo, L., Szoszkiewicz, R., Park, Y., Lee, S. Y., Iwamoto, T., Ferreira, L. C. S., & Tomich, J. M. (2015). Branched amphiphilic cationic oligo-peptides form peptiplexes with DNA: A study of their biophysical properties and transfection efficiency. *Molecular Pharmaceutics*. <http://doi.org/10.1021/mp500524s>
- ⁴⁹ Jia, Z., Whitaker, S. K., Tomich, J. M., & Chen, J. (2016). Organization and structure of branched amphipathic oligopeptide bilayers. *Langmuir*, 32(38), 9883–9891. <http://doi.org/10.1021/acs.langmuir.6b02421>
- ⁵⁰ Wang, J., Dlamini, D. S., Mishra, A. K., Theresa, M., Pendergast, M., Wong, M. C. Y., Mamba, B. B., Freger, V., Verliefde, A. R. D., & Hoek, E. M. V. (2014). A critical review


-
- of transport through osmotic membranes. *Journal of Membrane Science*, 454, 516–537. <http://doi.org/10.1016/j.memsci.2013.12.034>
- ⁵¹ Lee, K. P., Arnot, T. C., & Mattia, D. (2011). A review of reverse osmosis membrane materials for desalination — Development to date and future potential. *Journal of Membrane Science*, 370, 1–22. <http://doi.org/10.1016/j.memsci.2010.12.036>
- ⁵² Emadzadeh, D., Lau, W. J., Matsuura, T., Rahbari-Sisakht, M., & Ismail, A. F. (2014). A novel thin film composite forward osmosis membrane prepared from PSf-TiO₂ nanocomposite substrate for water desalination. *Chemical Engineering Journal*, 237, 70–80. <http://doi.org/10.1016/j.cej.2013.09.081>
- ⁵³ Li, D., Yan, Y., & Wang, H. (2016). Recent advances in polymer and polymer composite membranes for reverse and forward osmosis processes. *Progress in Polymer Science*, 61, 104–155. <http://doi.org/10.1016/j.progpolymsci.2016.03.003>
- ⁵⁴ Emadzadeh, D., Lau, W. J., Matsuura, T., Ismail, A. F., & Rahbari-Sisakht, M. (2014). Synthesis and characterization of thin film nanocomposite forward osmosis membrane with hydrophilic nanocomposite support to reduce internal concentration polarization. *Journal of Membrane Science*, 449, 74–85. <http://doi.org/10.1016/j.memsci.2013.08.014>
- ⁵⁵ Chen, L., Gu, Y., Cao, C., Zhang, J., Ng, J. W., & Tang, C. (2014). Performance of a submerged anaerobic membrane bioreactor with forward osmosis membrane for low-strength wastewater treatment. *Water Research*, 50, 114–123. <http://doi.org/10.1016/j.watres.2013.12.009>
- ⁵⁶ Ulbricht, M. (2006). Advanced functional polymer membranes. *Polymer*, 47(7), 2217–2262. <http://doi.org/10.1016/j.polymer.2006.01.084>
- ⁵⁷ Lalia, S. B., Kochkodan, V., Hashaiekeh, R., & Hilal, N. (2013). A review on membrane fabrication : Structure, properties and performance relationship. *Desalination*, 326, 77–95. <http://doi.org/10.1016/j.desal.2013.06.016>
- ⁵⁸ Chung, T.-S., Zhang, S., Wang, K. Y., Su, J., & Ling, M. M. (2011). Forward osmosis processes: Yesterday, today and tomorrow. *Desalination*, 287, 78–81. <http://doi.org/10.1016/j.desal.2010.12.019>
- ⁵⁹ Akpınar, E., Turkmen, M., Canioz, C., & Neto, A. M. F. (2016). Role of kosmotrope-chaotrope interactions at micelle surfaces on the stabilization of lyotropic nematic phases. *The European Physical Journal E*, 39(107). <http://doi.org/10.1140/epje/i2016-16107-5>
- ⁶⁰ Khan, S. H., Kramkowski, E. L., & Hoffmann, P. M. (2016). NaCl-Dependent ordering and dynamic mechanical response in nanoconfined water. *Langmuir*, 32, 10802–10807. <http://doi.org/10.1021/acs.langmuir.6b02535>

-
- ⁶¹ Liu, L., Kou, R., & Liu, G. (2016). Ion specificities of artificial macromolecules. *Soft Matter*, 13, 68–80. <http://doi.org/10.1039/c6sm01773h>
- ⁶² Moelbert, S., Normand, B., & Rios, P. D. L. (2004). Kosmotropes and chaotropes : Modelling preferential exclusion, binding and aggregate stability, *Biophysical Chemistry*, 112, 45–57. <http://doi.org/10.1016/j.bpc.2004.06.012>
- ⁶³ Andrushcchenko, V. V., Vogel, H. J., & Prenner, E. J. (2007). Optimization of the hydrochloric acid concentration used for trifluoroacetate removal from synthetic peptides. *Journal of Peptide Science*, 13, 37-43. <http://doi.org/10.1002/psc.793>
- ⁶⁴ Barros, S. D. M., Avila, L. A., Whitaker, S. K., Wilkinson, K. E., Sukthankar, P., Beltra, E. I. C., & Tomich, J. M. (2017). Branched Amphipathic Peptide Capsules: Different ratios of the two constituent peptides direct distinct bilayer structures, sizes, and DNA transfection efficiency. *Langmuir*, 33, 7096 – 7104. <http://doi.org/10.1021/acs.langmuir.7b00912>

Appendix A – Copyright Permissions



[Home](#) [Create Account](#) [Help](#)

 **ACS Publications** Most Trusted. Most Cited. Most Read.

Title: Thermally Induced Conformational Transitions in Nascent Branched Amphiphilic Peptide Capsules

Author: Pinakin Sukthankar, Susan K. Whitaker, Macy Garcia, et al

Publication: Langmuir

Publisher: American Chemical Society

Date: Mar 1, 2015

Copyright © 2015, American Chemical Society

[LOGIN](#)

If you're a **copyright.com** user, you can login to RightsLink using your copyright.com credentials. Already a **RightsLink** user or want to [learn more?](#)

PERMISSION/LICENSE IS GRANTED FOR YOUR ORDER AT NO CHARGE

This type of permission/license, instead of the standard Terms & Conditions, is sent to you because no fee is being charged for your order. Please note the following:

- Permission is granted for your request in both print and electronic formats, and translations.
- If figures and/or tables were requested, they may be adapted or used in part.
- Please print this page for your records and send a copy of it to your publisher/graduate school.
- Appropriate credit for the requested material should be given as follows: "Reprinted (adapted) with permission from (COMPLETE REFERENCE CITATION). Copyright (YEAR) American Chemical Society." Insert appropriate information in place of the capitalized words.
- One-time permission is granted only for the use specified in your request. No additional uses are granted (such as derivative works or other editions). For any other uses, please submit a new request.

If credit is given to another source for the material you requested, permission must be obtained from that source.

[BACK](#)[CLOSE WINDOW](#)

Copyright © 2017 [Copyright Clearance Center, Inc.](#) All Rights Reserved. [Privacy statement](#). [Terms and Conditions](#). Comments? We would like to hear from you. E-mail us at customer@copyright.com



RightsLink®

Home

Create Account

Help



Title: Organization and Structure of
Branched Amphipathic
Oligopeptide Bilayers
Author: Zhiguang Jia, Susan K.
Whitaker, John M. Tomich, et al
Publication: Langmuir
Publisher: American Chemical Society
Date: Sep 1, 2016

Copyright © 2016, American Chemical Society

LOGIN

If you're a **copyright.com** user, you can login to RightsLink using your copyright.com credentials. Already a **RightsLink** user or want to [learn more?](#)

PERMISSION/LICENSE IS GRANTED FOR YOUR ORDER AT NO CHARGE

This type of permission/license, instead of the standard Terms & Conditions, is sent to you because no fee is being charged for your order. Please note the following:

- Permission is granted for your request in both print and electronic formats, and translations.
- If figures and/or tables were requested, they may be adapted or used in part.
- Please print this page for your records and send a copy of it to your publisher/graduate school.
- Appropriate credit for the requested material should be given as follows: "Reprinted (adapted) with permission from (COMPLETE REFERENCE CITATION). Copyright (YEAR) American Chemical Society." Insert appropriate information in place of the capitalized words.
- One-time permission is granted only for the use specified in your request. No additional uses are granted (such as derivative works or other editions). For any other uses, please submit a new request.

If credit is given to another source for the material you requested, permission must be obtained from that source.

BACK

CLOSE WINDOW

Copyright © 2017 Copyright Clearance Center, Inc. All Rights Reserved. [Privacy statement](#). [Terms and Conditions](#).
Comments? We would like to hear from you. E-mail us at customercare@copyright.com